



High Band Neutrino Beam for Tev II
P. Spillantini

1/23/81

1 Introduction

This note describes the feasibility of developing a well collimated parent hadron beam with a high collection efficiency for higher energy hadrons- a collection efficiency greater than 50% for hadron momenta above 400 GeV/c. The focussing device for this beam would be a super-conducting horn. Two observations (described in Section 2) were applied to design the horn that, on paper, would produce a highly collimated beam (described in section 3). Normally the feasibility of a new device depends on the particulars of a project; the horn design should arouse crucial criticisms that would condition its final technical development. The horn will be limited to slow spill applications because of beam effects on the materials and cooling fluids.

The merits of the beam are discussed in Section 4. In particular a discussion is given about the possibility of using a 1000m decay tunnel, and also the possibility of using the muons from pi decay for a muon beam.

2 (1.1) Collection of a Wide Momentum Band

Two observations can be made about the collection of particles from a target:

In the thin lens approximation, a single lens is able to focus a wider momentum band than any focusing-defocusing or defocusing-focussing system (See figure 1 and Appendix 1). This implies that a horn is able to focus a wider momentum band than any quadrupole lens system.

Furthermore, if we relax the thin lens approximation, the focussed momentum band can be made even wider. In thin lens, the focusing is done by a field whose strength is proportional to the distance R at which the particle enters the lens. If $L(R)$ is the path length of the particle inside the lens and $B(R)$ is the field strength then $L(R)*B(R)=cR$ in the thin lens case. Indeed, for a horn, we could contour the field and path length in different ways to approximate the thin lens case. For example,

$$\begin{array}{ll}
 B(R) = k \cdot R & \text{if } L = \text{constant} \\
 B(R) = \text{constant} & \text{if } L = L \cdot R \\
 B(R) = k/R & \text{if } L = L \cdot R^{**2} \ll 1
 \end{array}$$

In general, if $B(R) = k \cdot R^{**2}$ with $\textcircled{1}$ the path of the particle in the magnetic field increases with R as $L(R) = L \cdot R^{**2}$; therefore, if $P > \bar{P}$ is the focussed momentum, particles with p greater than \bar{P} tend to leave the field later than particles with $p = \bar{P}$ and hence undergo extra focussing. The same happens to particles with p less than \bar{P} , which leave the lens earlier. This effect, negligible in the thin lens approximation, becomes effective as the thickness of the lens increases with respect to the focal length z (See figure 2). Naturally, only shapes of the kind shown in figure 2 are effective, while shapes such as those given in figures 3b and 3c are much less convenient. In principle it should be possible to find a function $B(R)$, [or possibly $B(R, Z)$] that will focus all momenta, but in practice the field should weaken so strongly with increasing R and/ or Z that the length of the focussing system would be enormous; high momentum particles would never be able to leave the lens. However, when the ratio of the path length and Z is as much as 10, a shape of $B(R) = c_1/R + c_2/R^{**2}$ widens the momentum acceptance by a factor of four or five over the thin lens case. Since a field $B(R) \propto R^{-2}$ is technically difficult to achieve, a shape of $B(R) \propto R$ is the most reasonable one to consider.

3 1.1.1 A well collimated high band parent hadron beam

These concepts were applied to the problem of fabricating a parent hadron beam for Tevatron II. Choosing $Z=5$ m and $L=10$ m for the length of the focussing lens, we can achieve a focussing effect as shown in figure 4, where the exit angle is plotted as a function of the entrance angle for various momenta. As can be seen in this figure, particles are focussed at different \bar{P} depending on θ : $P > = 600$ GeV/c for $\theta = 0.2$ mrad till $\bar{P} = 600$ GeV/c for $\theta = 1$ mrad. "

A schematic of a section of such a lens is sketched in figure 5. The guiding idea is to put the s.c. wire in good thermal and electrical contact with a metallic core, which should also provide a stable mechanical support for the wire turn. The residual proton beam passes through the center without touching any element of the device. The azimuthal acceptance is given in figure 6, from which it can be seen that some percent of the particles produced would strike the super conducting wire. Indeed an absorber, with the same shape as the metallic bore, should be placed in front of the

lens to protect the s.c. wire. The absorber should not be in thermal contact with the helium bath to avoid boiling. (See fig. 7) To avoid absorption of wrong momentum and wrong sign particles in the surrounding bore, with consequent boiling of the helium, the lens must be divided into sections, with absorbers interleaved between them. For the limited length of the proposed lens a division into two sections with an absorber between them would be sufficient (See figure 7).

The choice of the total length of the lens is a compromise: Since the ratio between the path length of the particles inside the lens and the focal length Z is around 1, the accepted momentum band is only a factor of two greater than the thin lens case (See again figure 4); but, in this manner, the contribution of the beam divergence at the exit of the lens to the beam dimension at the end of the decay tunnel is negligible.

The lens is supposed to carry a total current of 10 kA; if the total cross section of the s.c. wires is 9 mm, the current density will be 1100 A/mm, well within the specifications of commercial s.c.wires. The resulting magnetic field will be $B=0.50$ Tesla from $R=0.002$ m to $R=0.004$ m and $B(R)=0.2/R$ for $R > 0.004$ m.

Two collimators (C_1 and C_2 in figure 7) cut the low momentum particles and define the geometry of the beam. Moreover, a reflector is added downstream from the magnetic lens to improve the focussing. It profits of the fact that the lens (given the $B(R)$ dependence of the field) focusses particles of the same momentum in a circular ring, irrespective of the entrance angle; at a suitable distance from the lens particles leaving with a different momentum pass at different distances from the axis and can be handled independantly.

For the parent hadron beam, the accepted momentum band is very wide (See figure 8), and the focussing is very good (See figure 9). This parent beam gives the high band neutrino spectrum of figure 10, compared in figure 11 and 12 with the bare target and perfect focussing cases. The muon momentum spectrum is given in figure 13 and their radial distribution is reported in figure 14.

4 **h1 4** Conclusions Some interesting consequences of realizing a highly collimated high band parent hadron beam must be pointed out:

1) Muons from K decay have a large divergence and can therefore be detected outside the hadron beam. This leads to the possibility of tagging the high energy part of the neutrino spectrum ($E_\nu > 1/4 E_p$).

2) The small radial dimensions of the parent beam make the tagging very clean and clear. In fact, the strong angular correlation between the nu-event and the detected muon (See figure 16), together with the time coincidence should avoid any ambiguity in a not too sophisticated tagging system.

3) The most energetic muons come from pi decay. They give a narrow spot at the end of the decay tunnel, only a little larger than that given by the parent hadron beam (See again figure 14). Why should we lose these muons and waste 1 km of shielding for them?

Could they be bent (together with the residual proton and hadron beams) and be used for physics?

4) If the answer is yes, why not do the bending at the end of a longer tunnel (for example 1000m long)?

The total fluxes of muons and neutrinos would increase proportionally. The less energetic muons are much more open in angle and absorbed in the residual shielding.

In figure 17, 18, 19 and 20 are given the muon and neutrino spectra and the pi, K, and muon radial distributions assuming the length of the decay tunnel is doubled. In figure 21, an example of a simple tagging device is reported.

Finally in figures 22, 23, and 24 are given the neutrino spectra and the hadron and muon radial distributions for the standard 500 m decay tunnel, but increasing the scale of the lens and collimators by a factor of two. This shows that diminishing the current density by a factor of four, or increasing the size of the lens to avoid radiation damage, does not drastically deteriorate the quality of the hadron or neutrino beams.

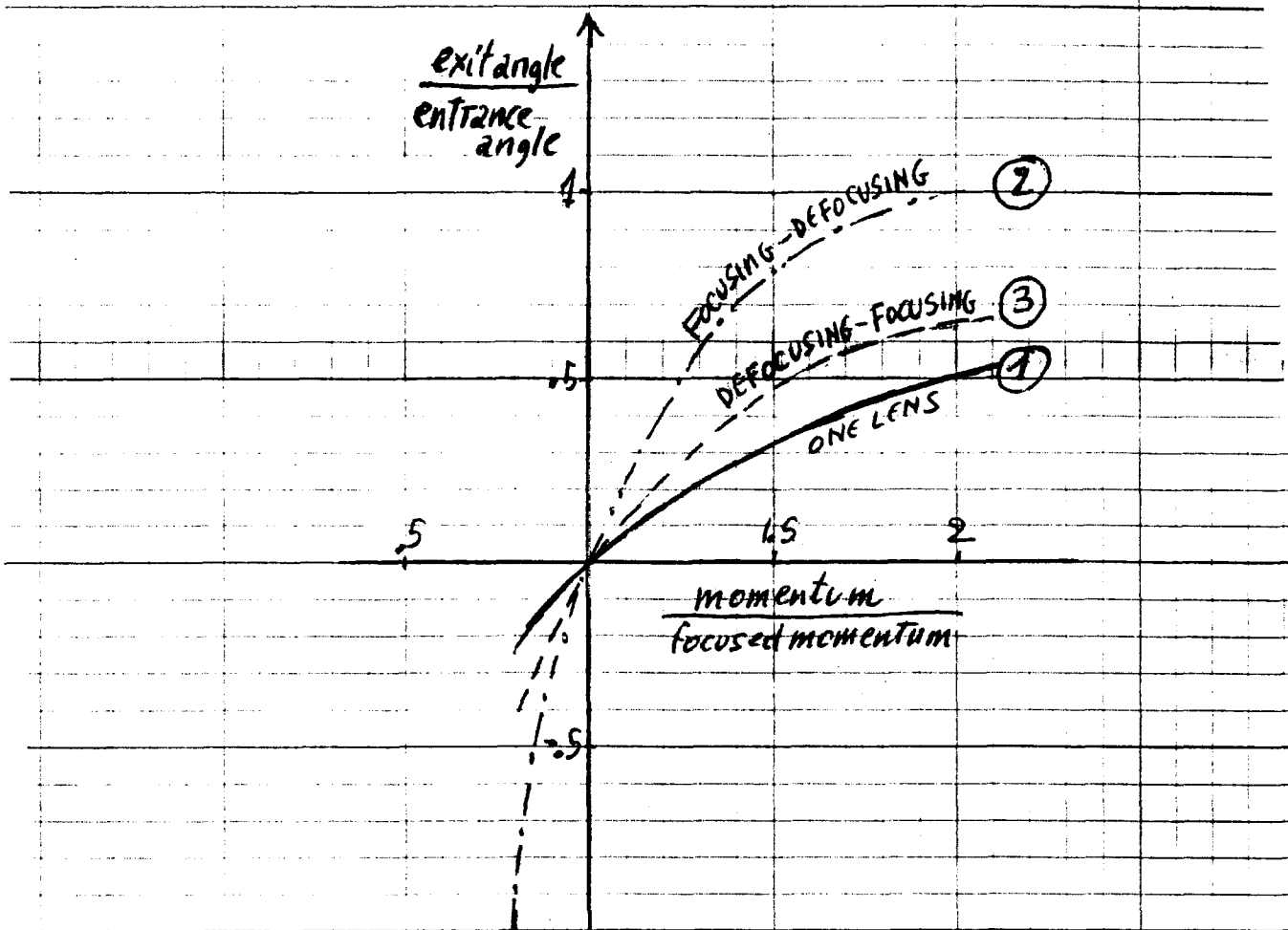


FIGURE 1

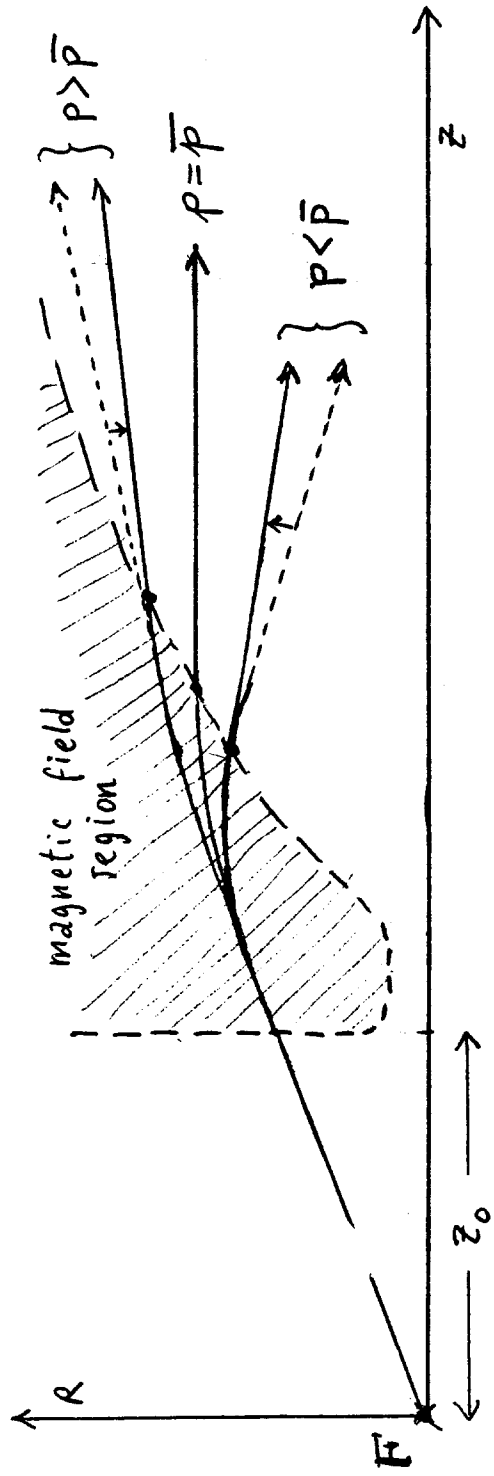
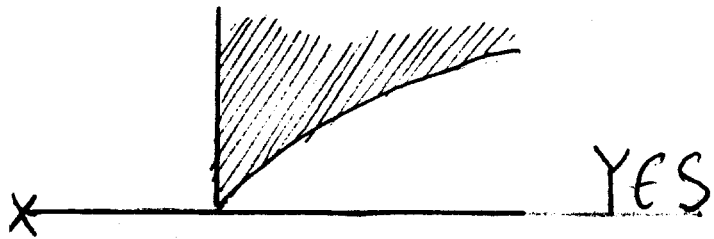
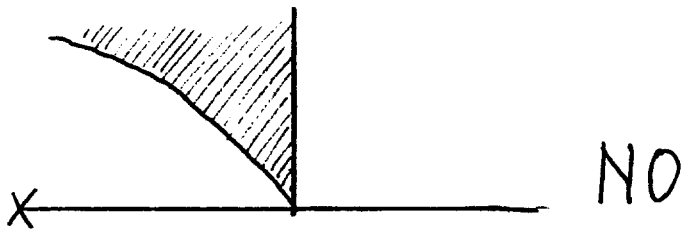


Fig 2

a)



b)



c)

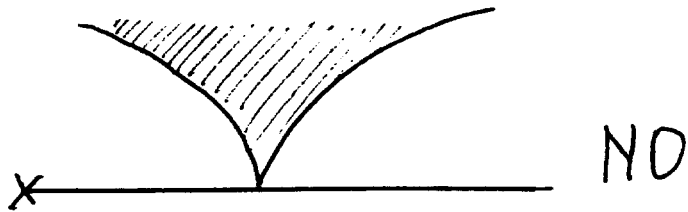


Fig 3

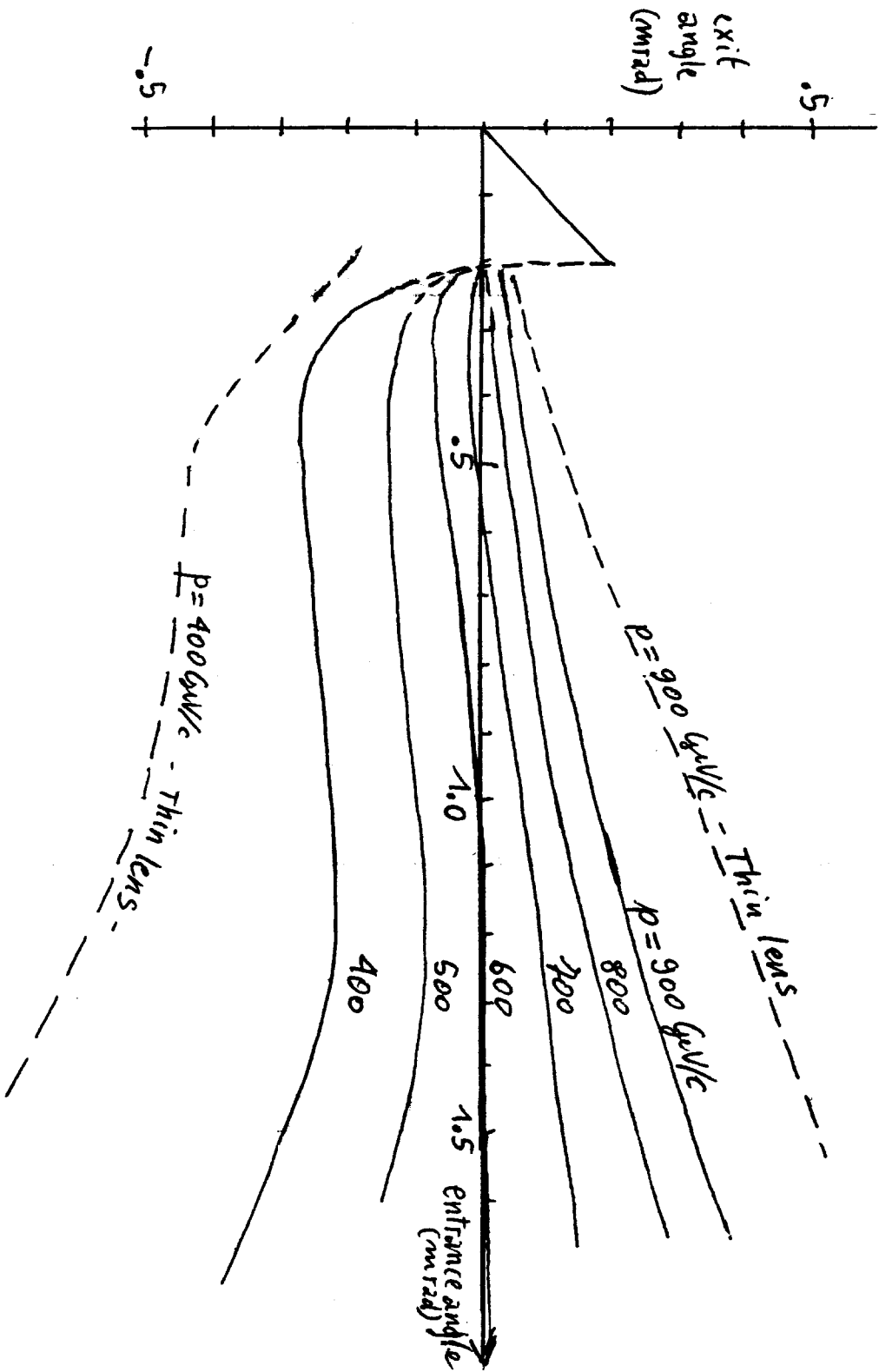
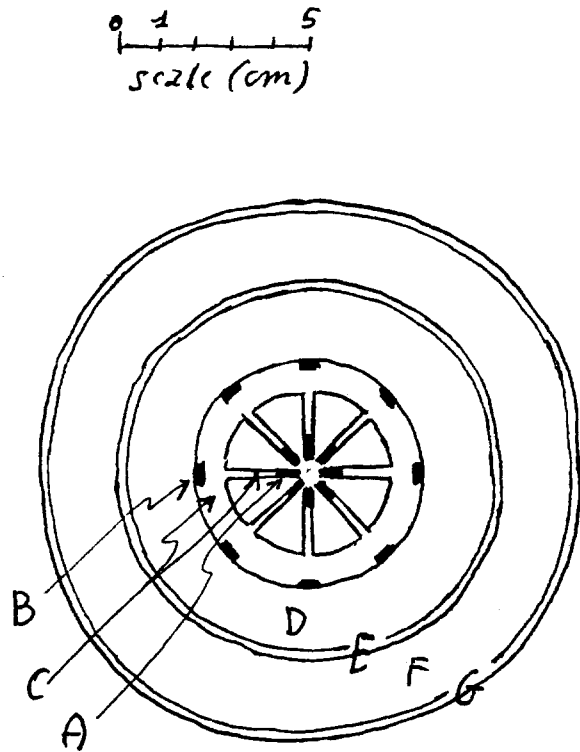
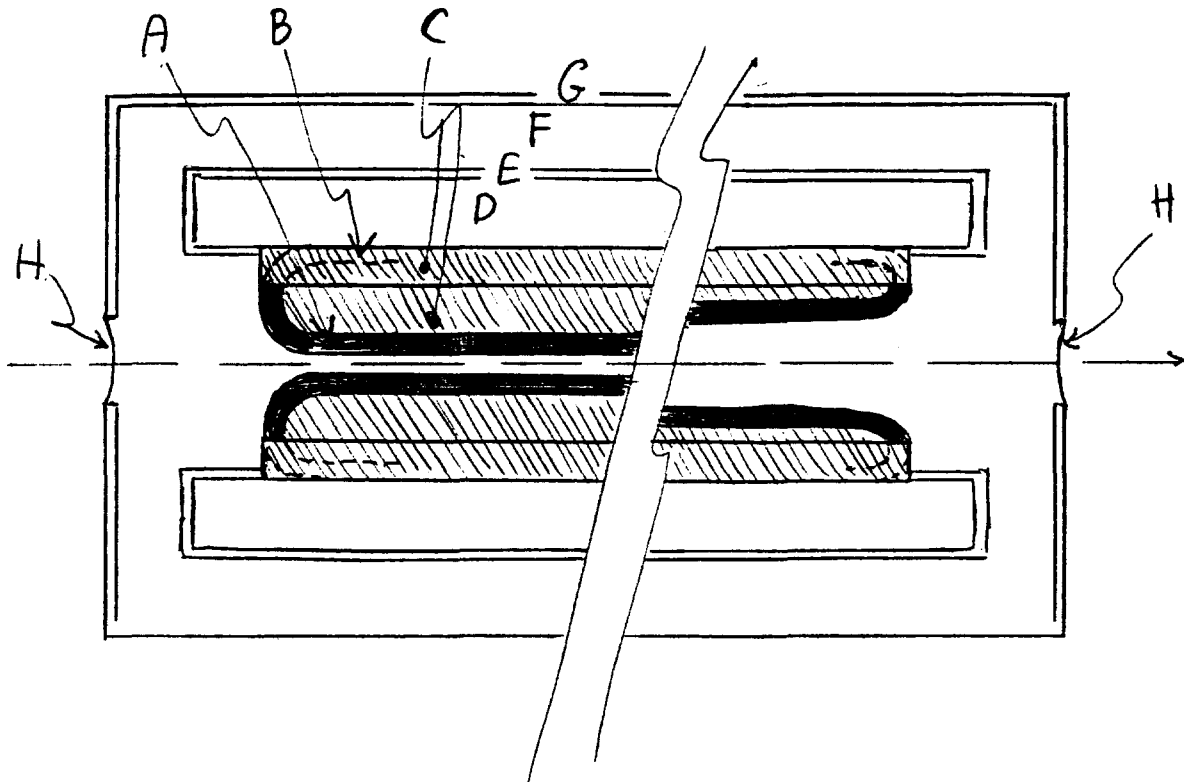


Fig 4

FIGURE 5



- A = Superconducting wire producing the toroidal field.
- B = Return of the s.c. wire.
- C = Metallic Bore (Cu or Al) with small wings arriving till near the center. To these wings are welded the s.c. wires, in thermal and electrical contact with the bore through them.
- D - Liquid Helium bath.
- E - Liquid Helium tank.
- F - Thermal shielding in vacuum.
- G - Vacuum tank.
- H - Thin windows for the particles.



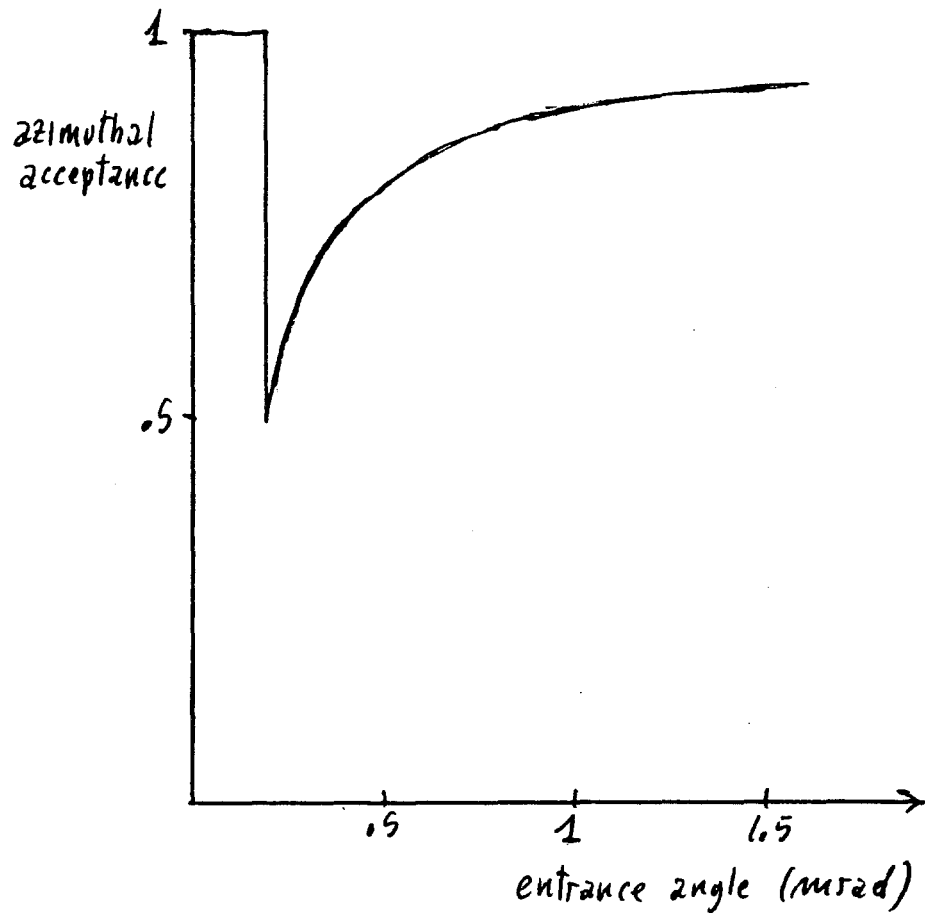


FIGURE 6

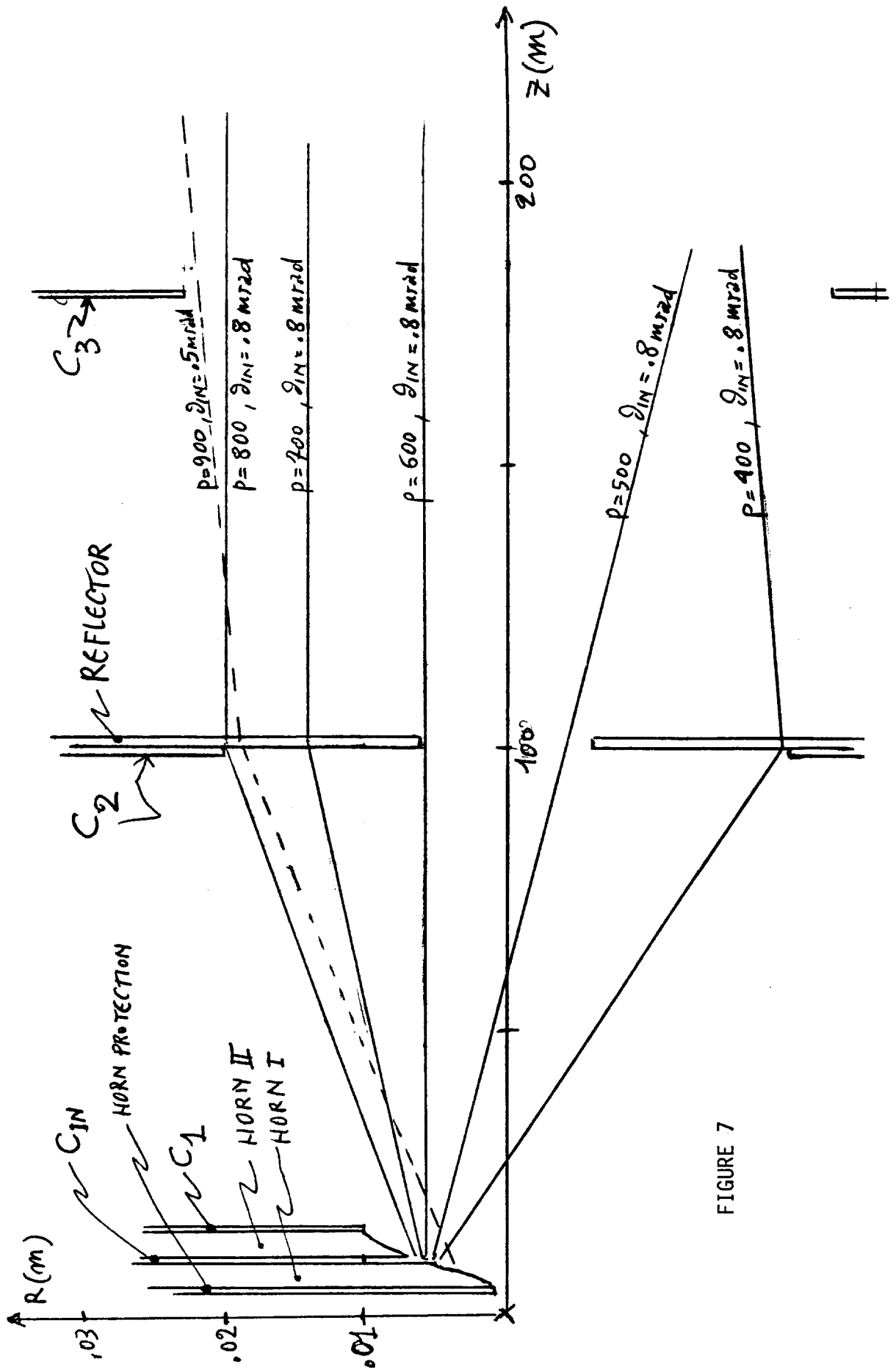


FIGURE 7

HADRONS / (GeV X INTERACTING PROTON)

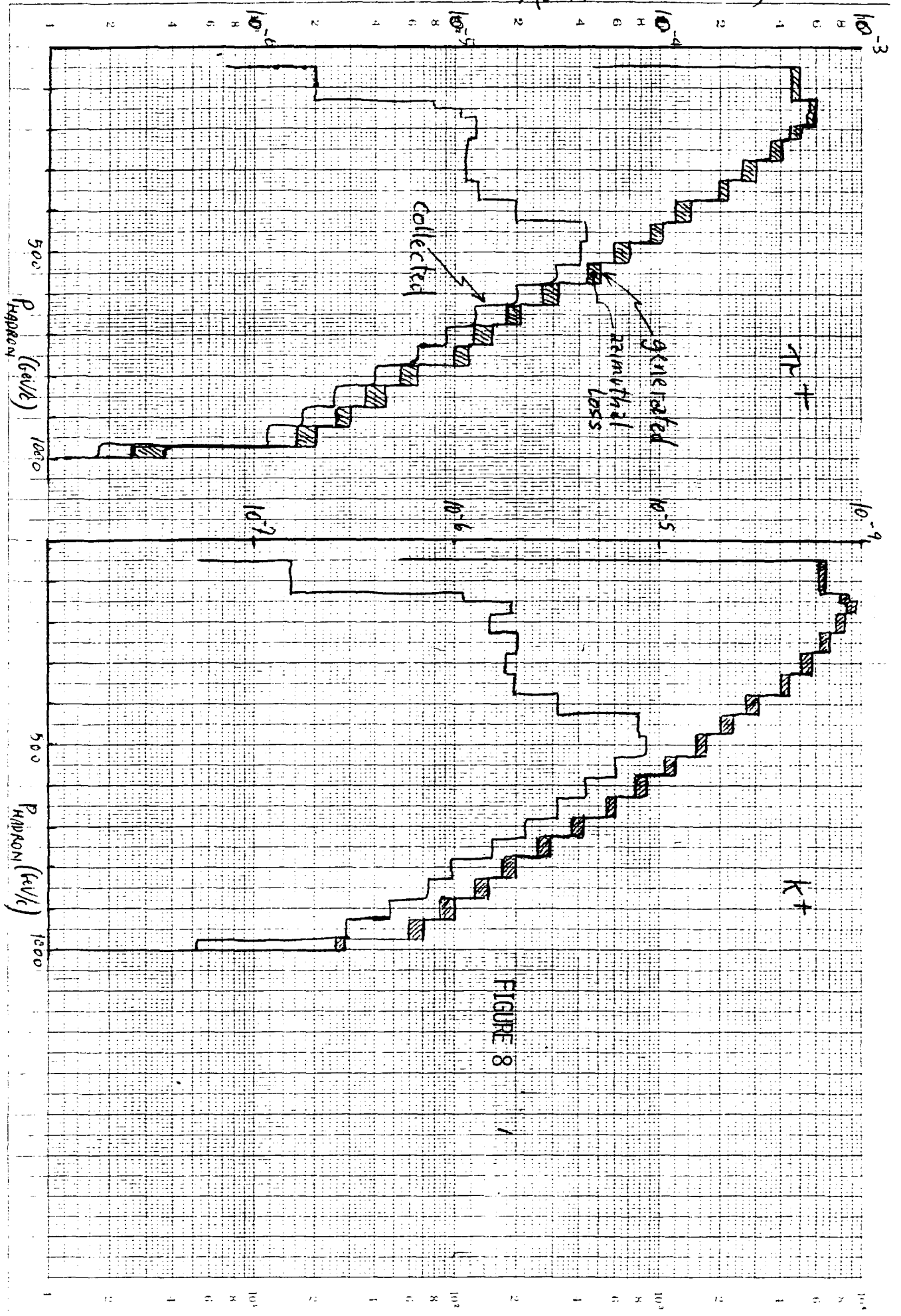


FIGURE 8

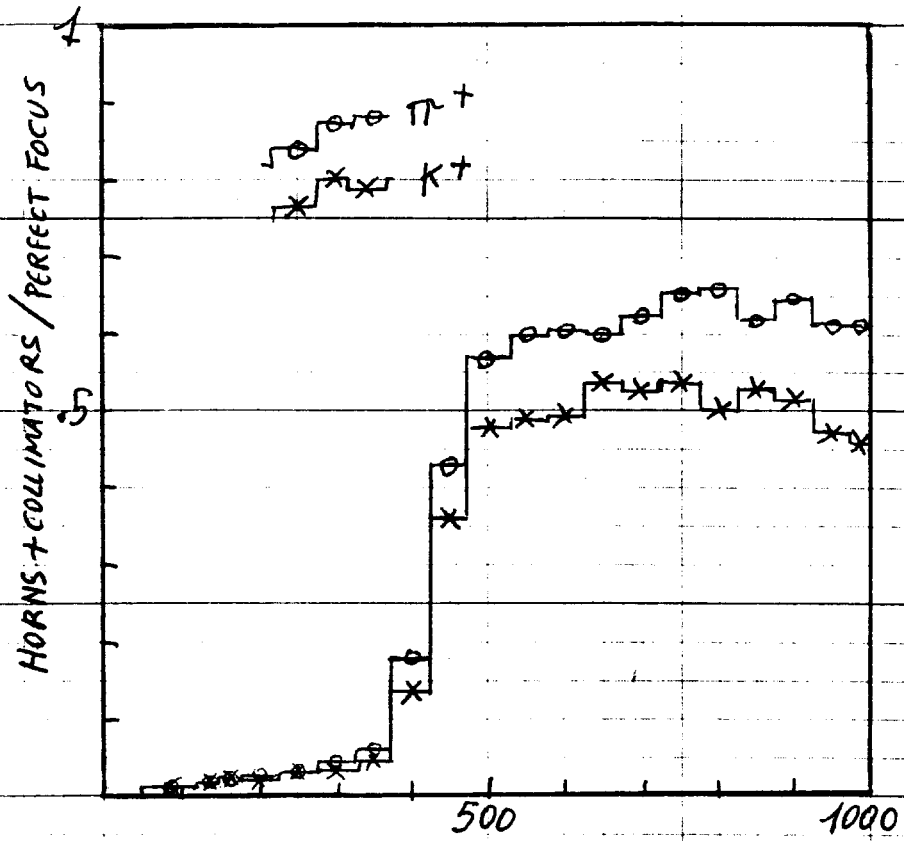


FIGURE 8B

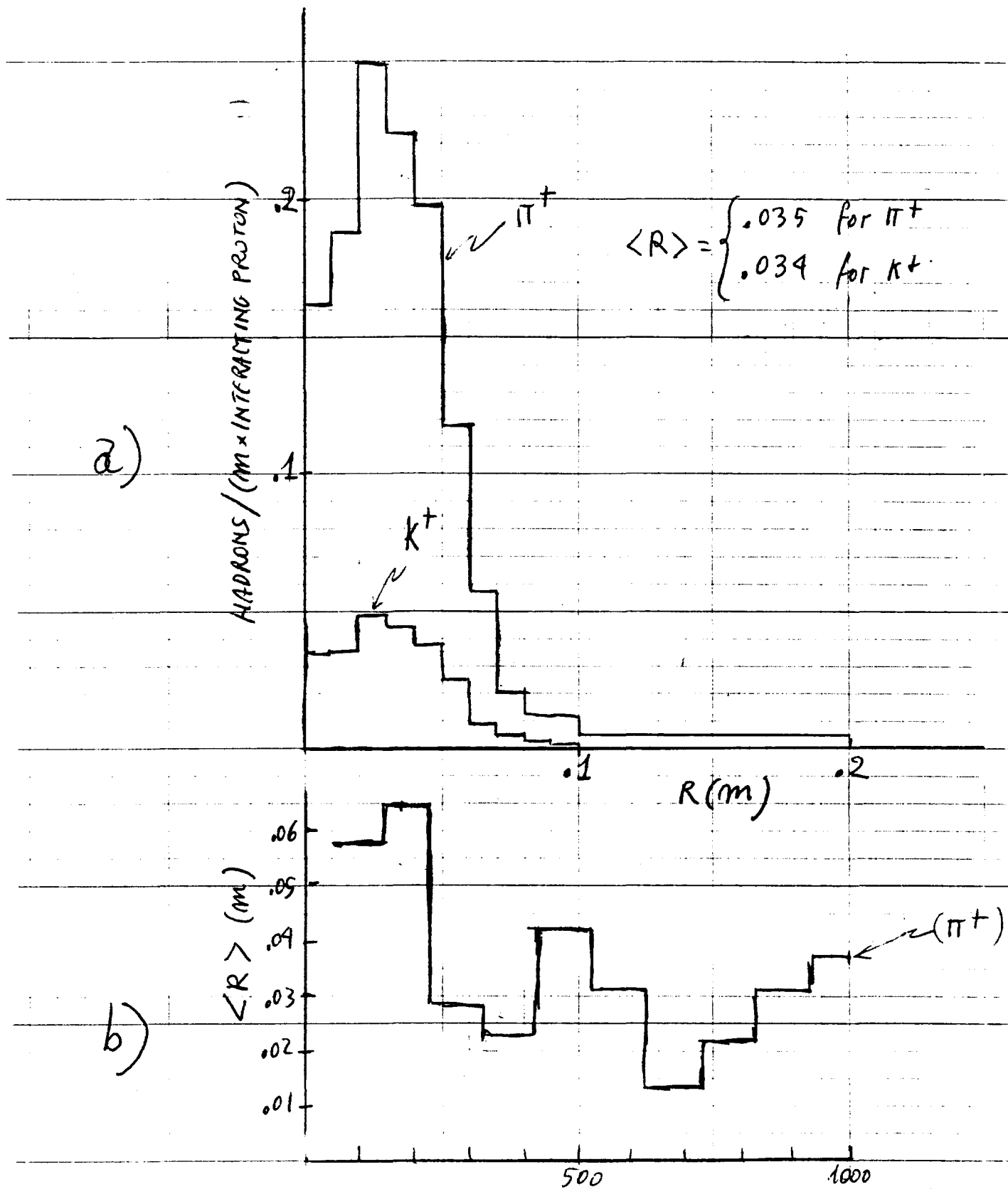


FIGURE 9

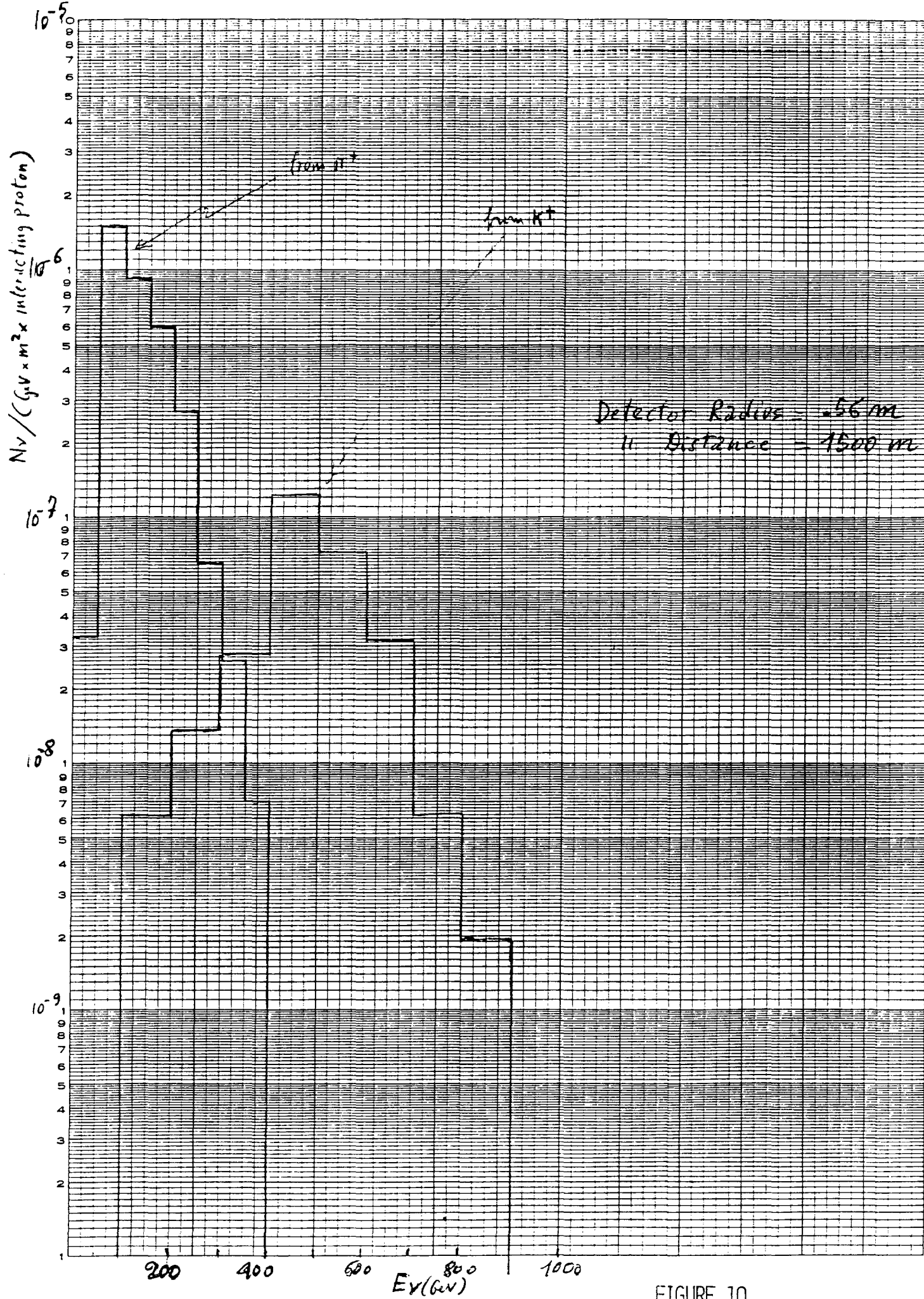


FIGURE 10

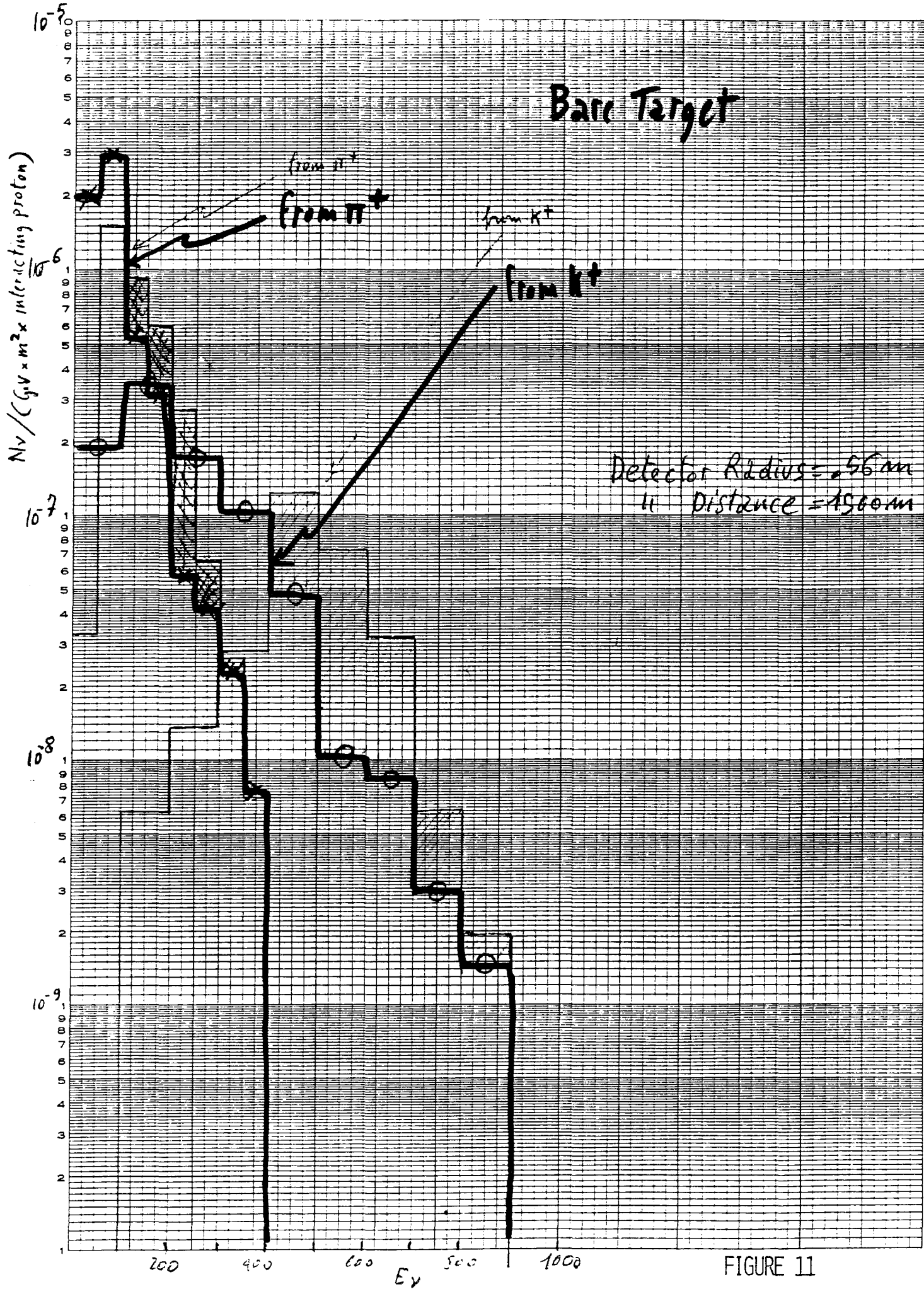


FIGURE 11

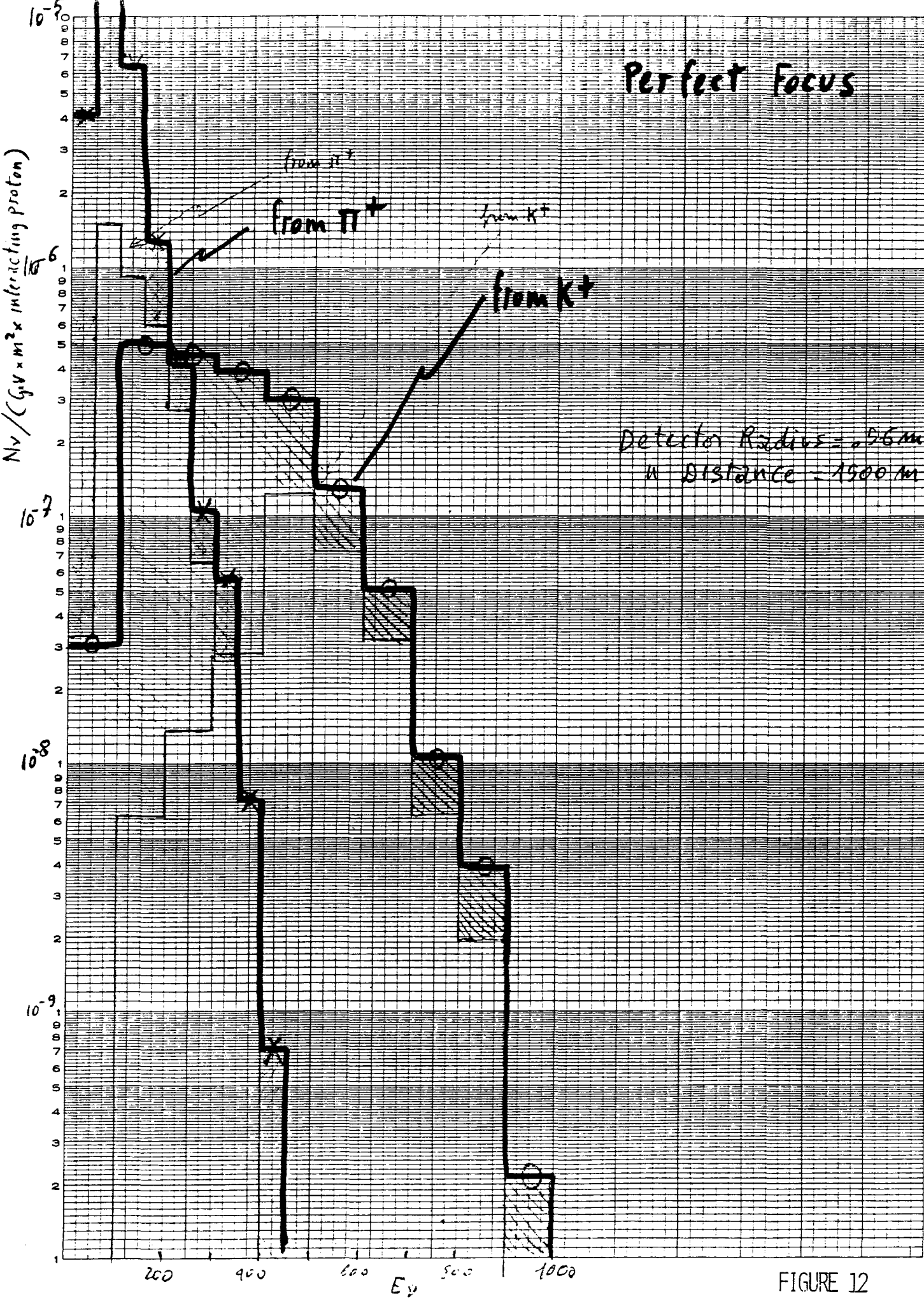
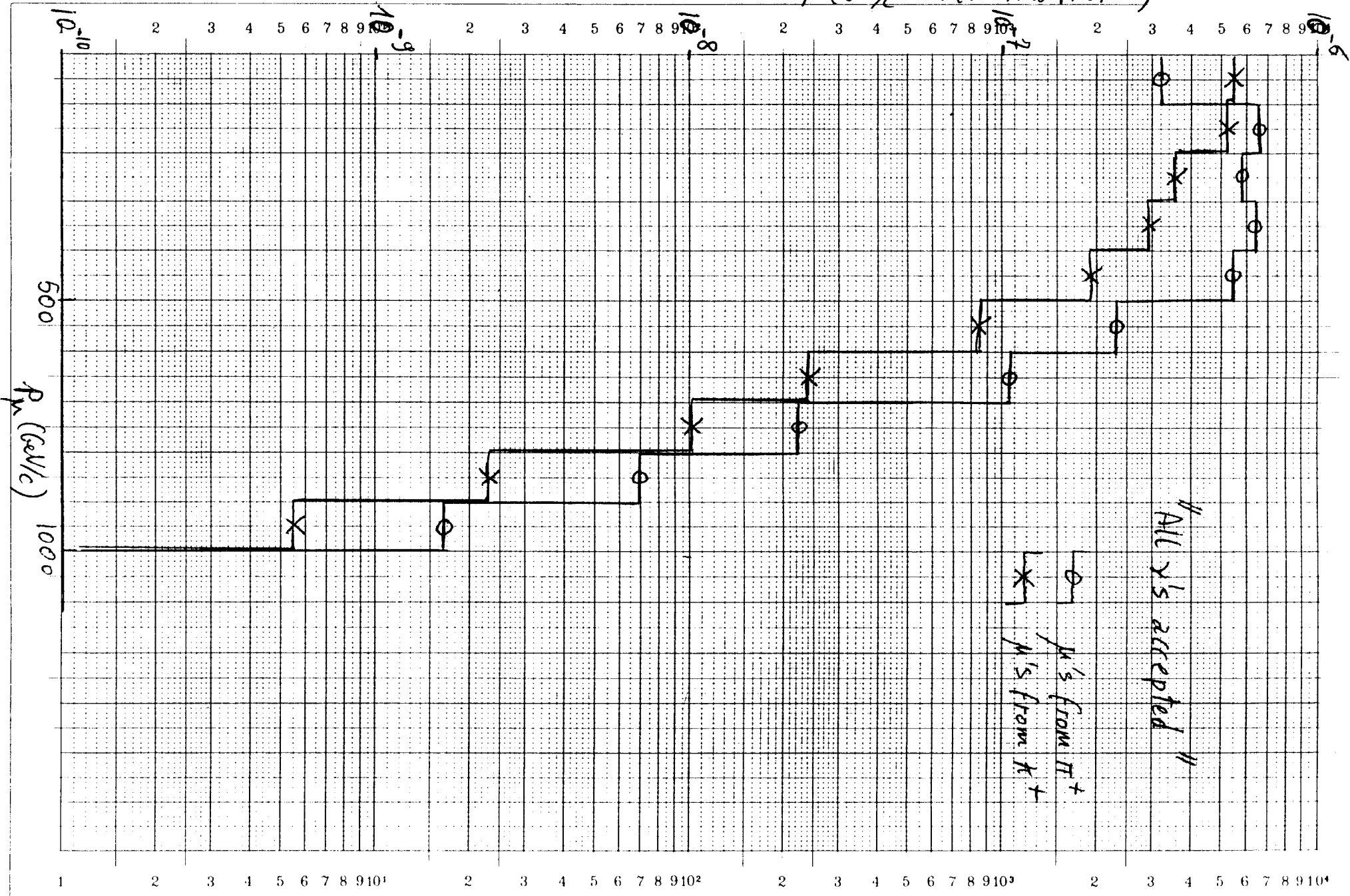


FIGURE 12

MUONS / (GeV/c x INTERACTING PROTON)



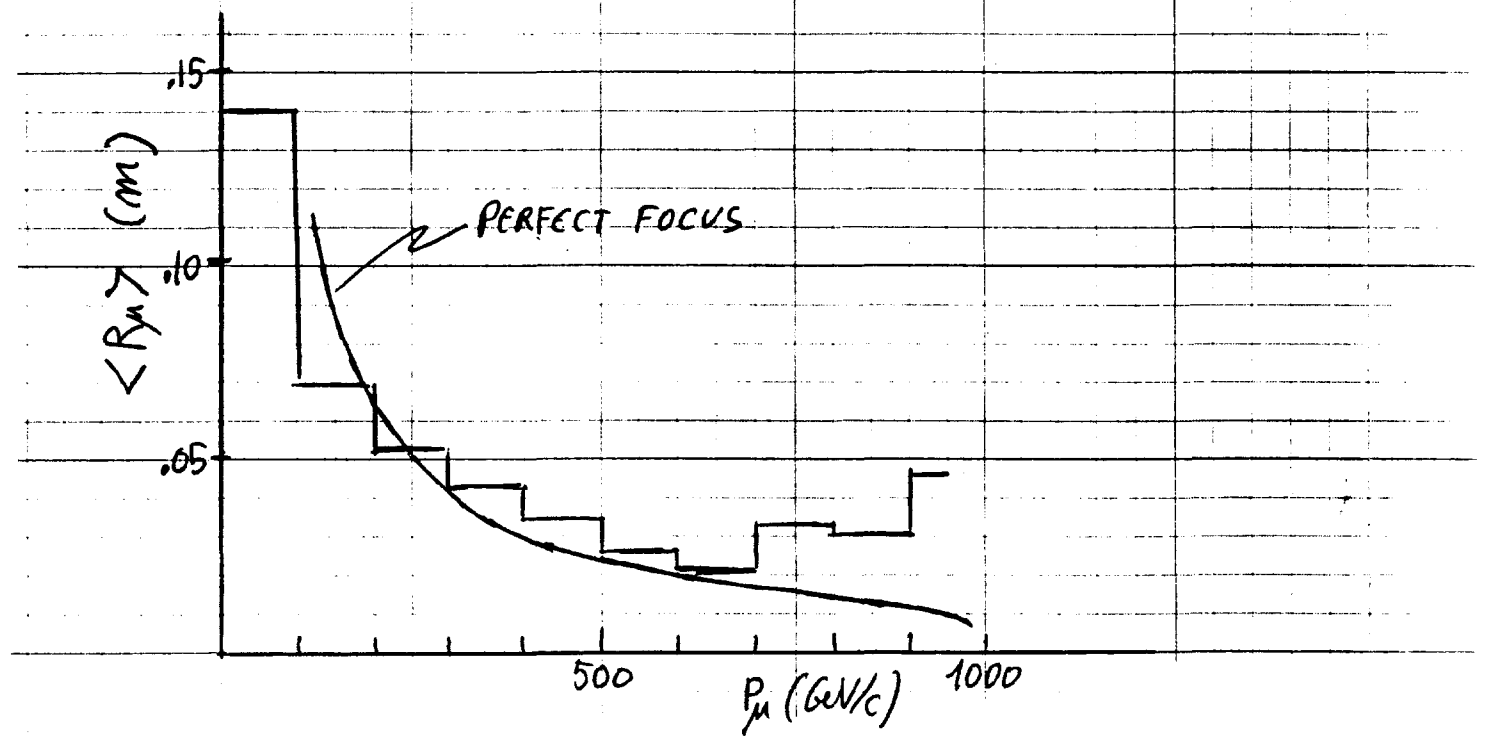
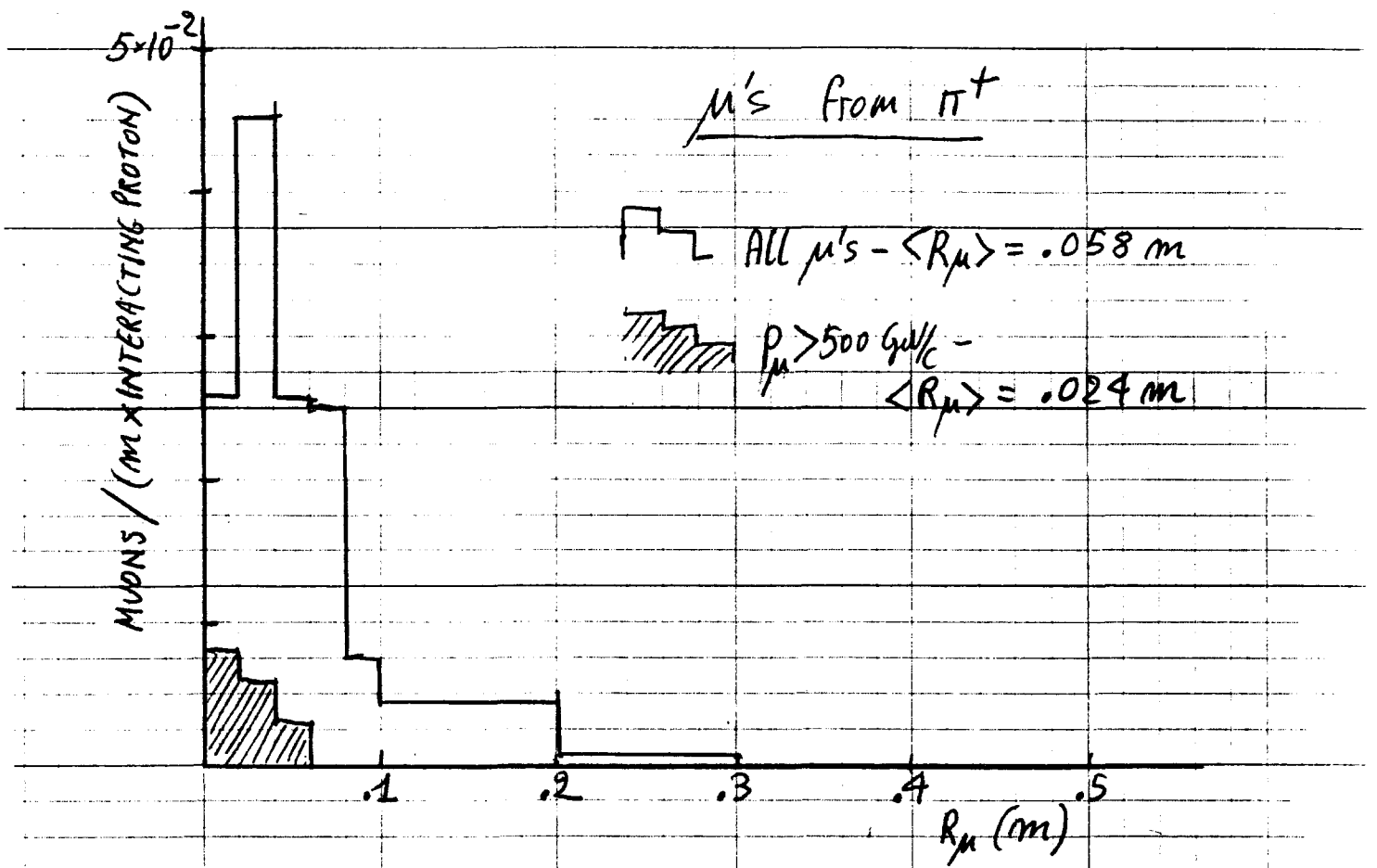


FIGURE 14

Fraction of μ 's in a $\Delta\theta_\mu \times \Delta P_\mu$ box

		θ_μ (mrad) \rightarrow					
		0-.2	.2-.4	.4-.6	.6-.8	.8-1.0	1.0-2.0
P_μ (GeV/c) \downarrow	0-100	0	.001	0	0	.003	.283
	100-200	0	.001	.007	.003	.009	.226
	200-300	0	0	.012	.031	.067	.057
	300-400	0	.007	.040	.092	.013	0
	400-500	.009	.024	.051	.004	0	0
	500-600	.012	.020	.006	0	0	0
	600-700	.005	.004	.001	0	0	0
	700-800	.002	.002	0	0	0	0
	800-900	.001	0	0	0	0	0
	900-1000	0	0	0	0	0	0
		0					
	0-1000	.030	.060	.116	.131	.092	.568

μ 's from K^+ - "All ν 's accepted"

FIGURE 15

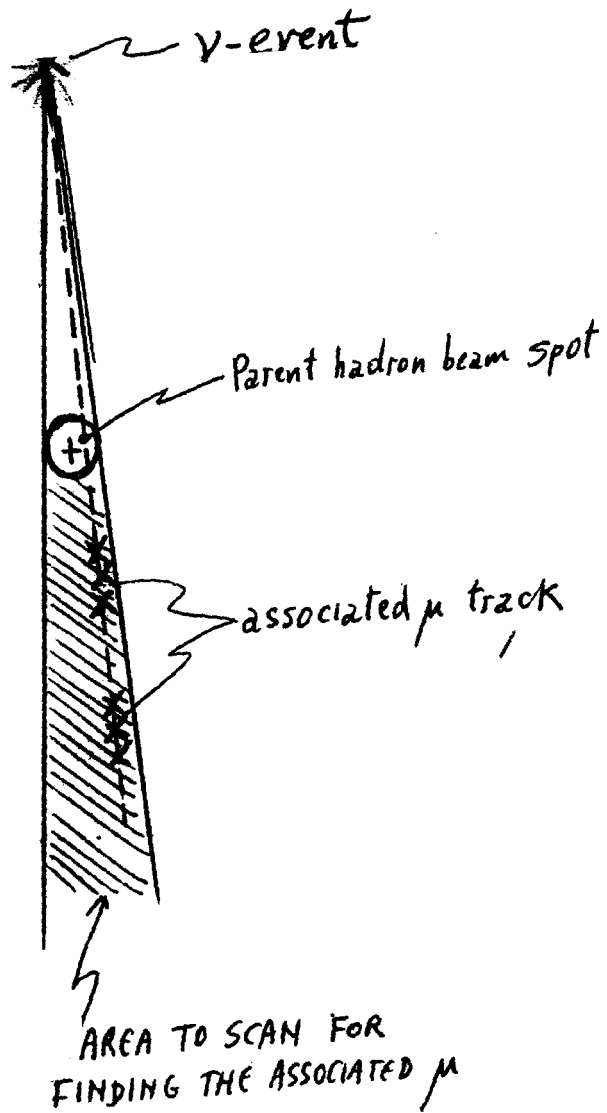


FIGURE 16

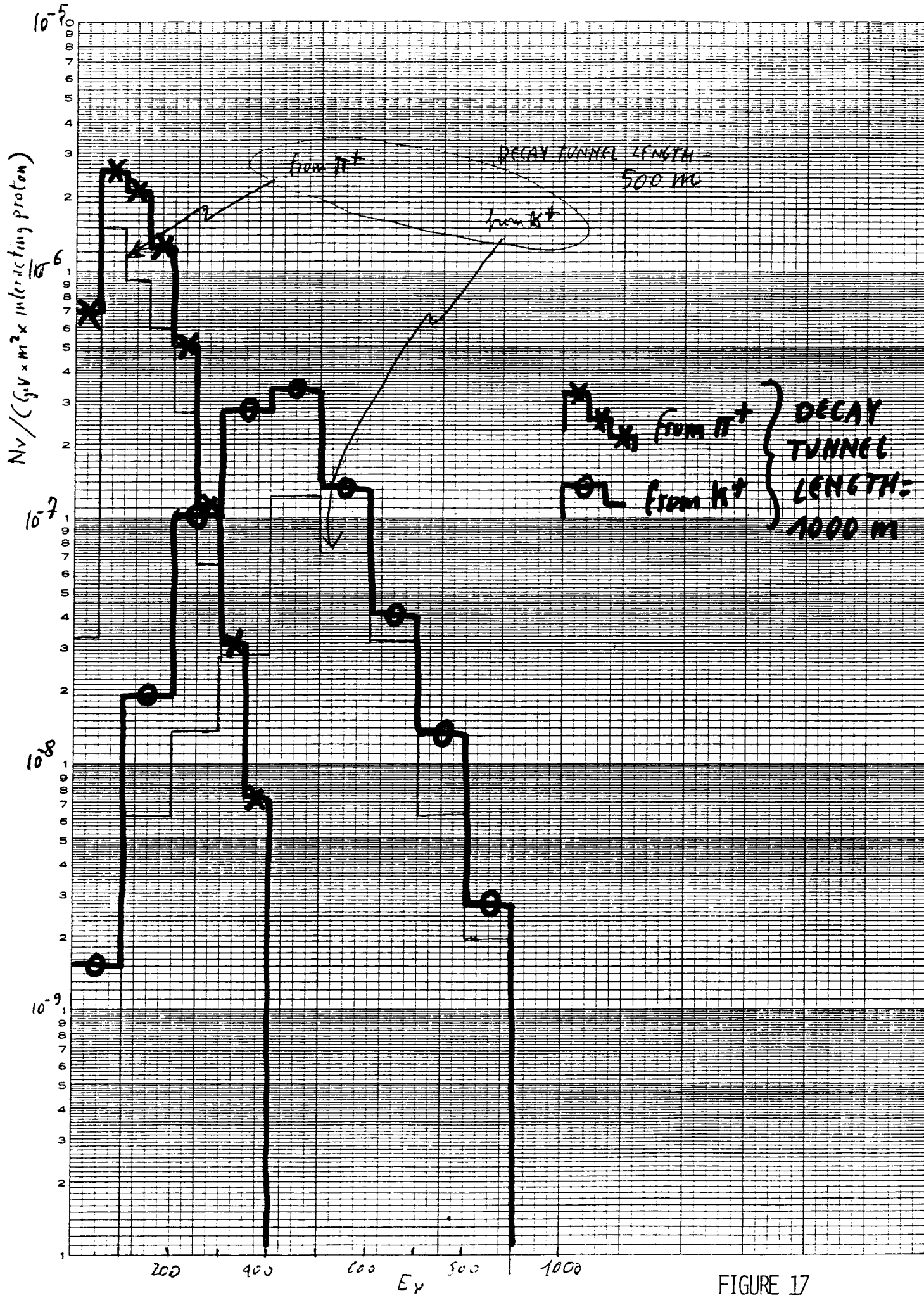
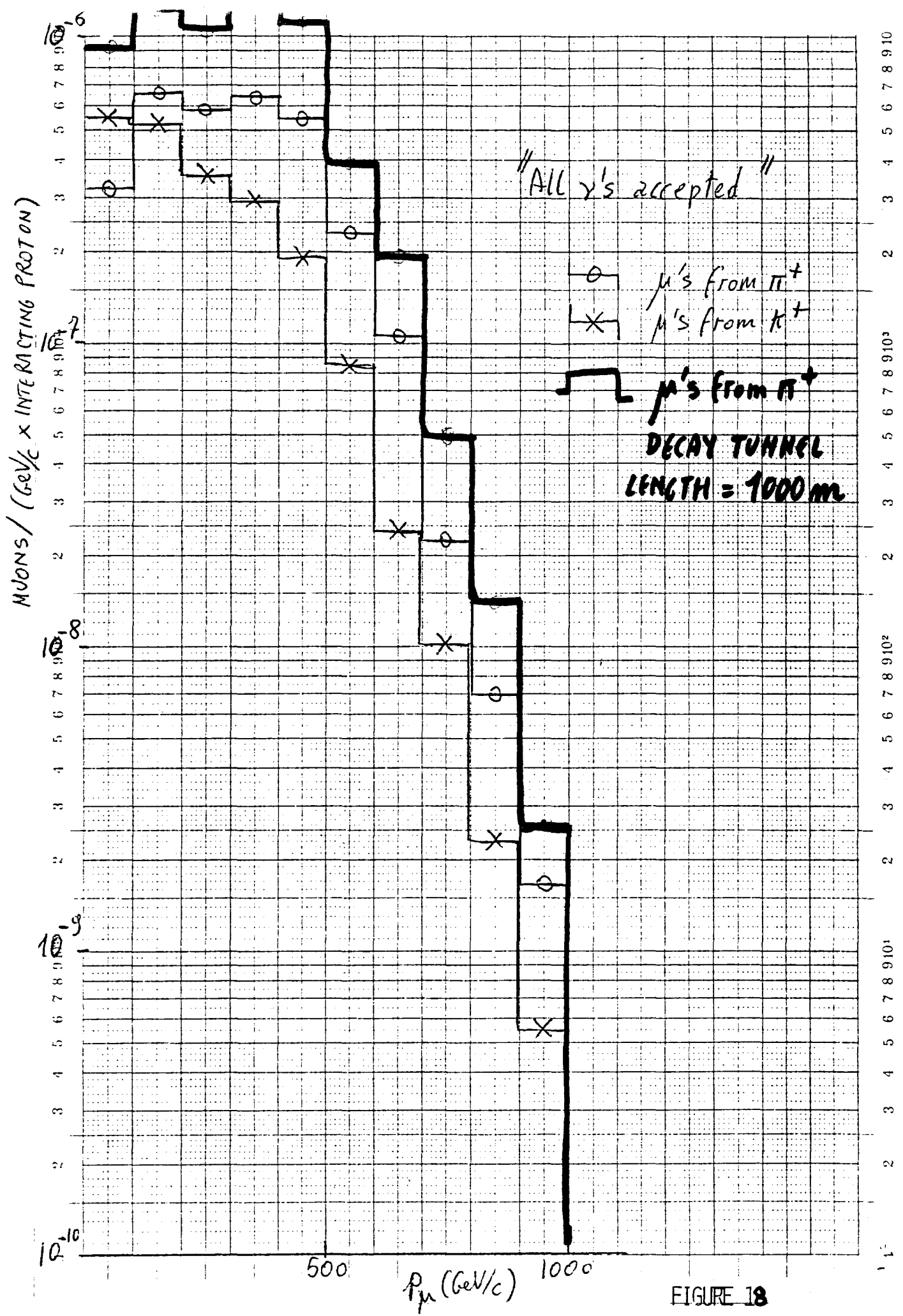
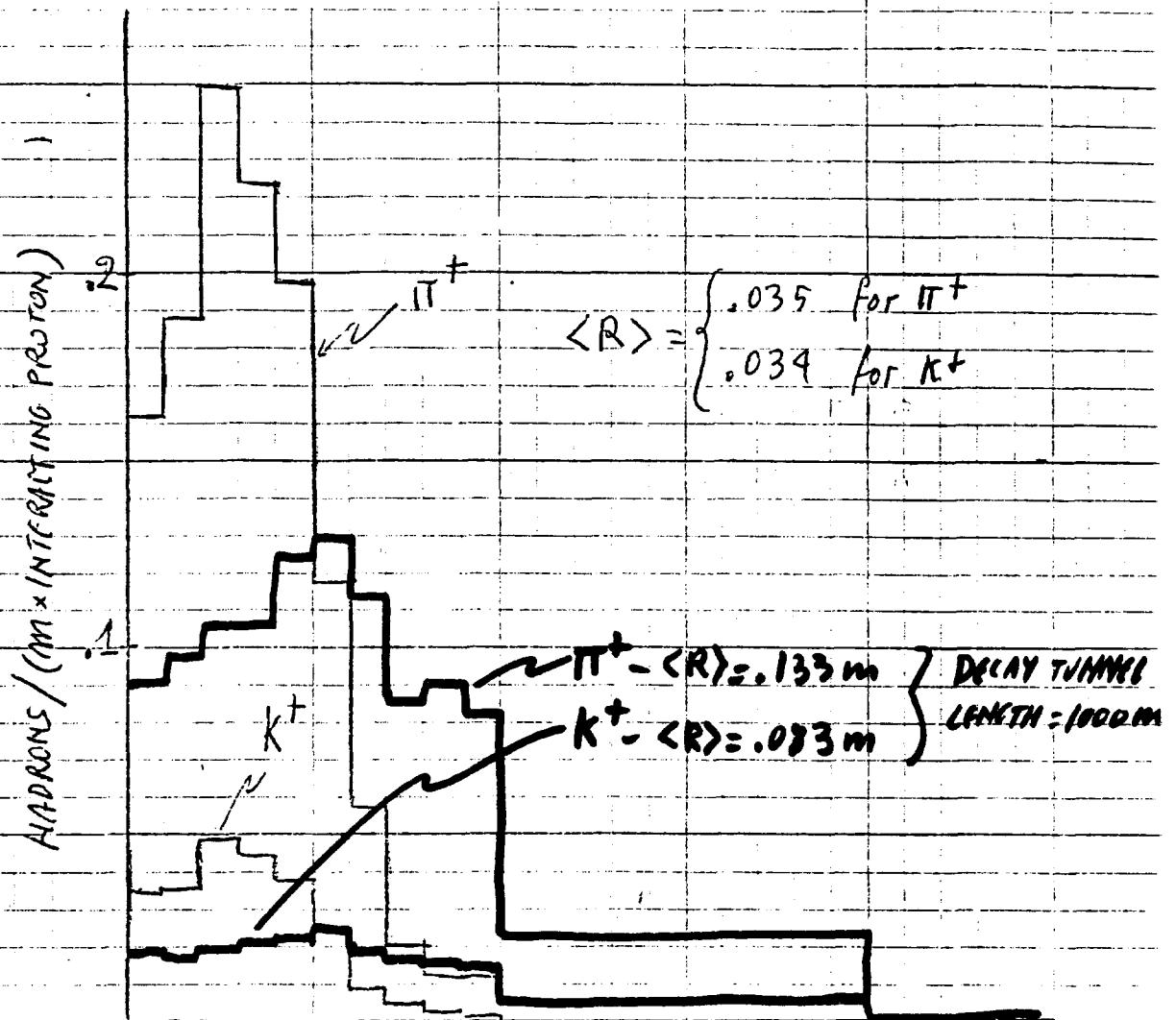


FIGURE 17



a)



b)

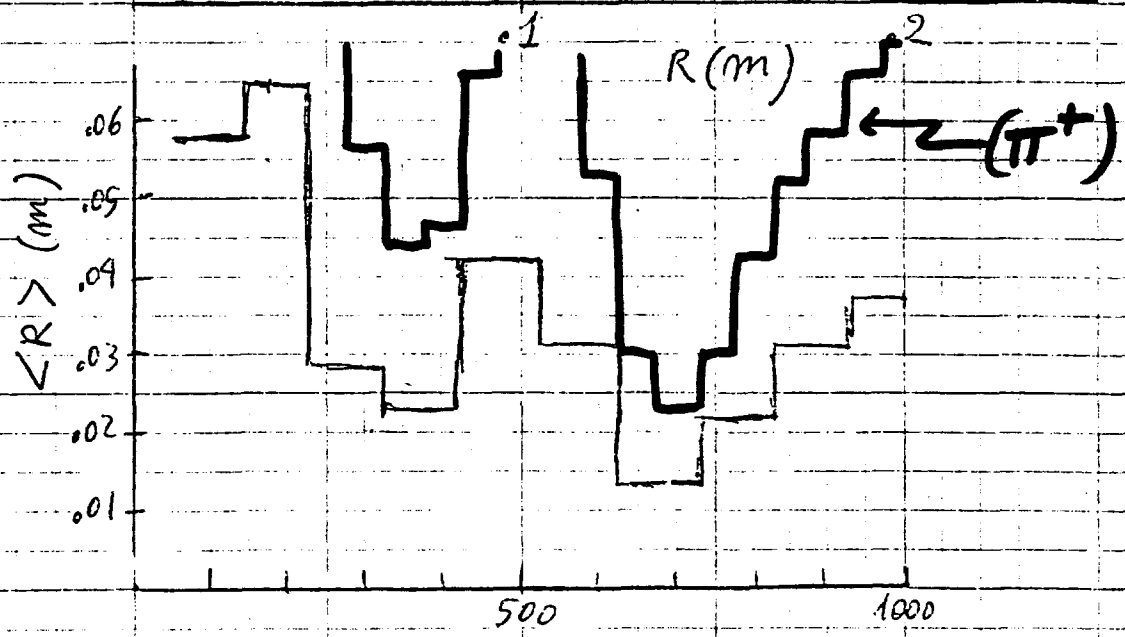


FIGURE 19

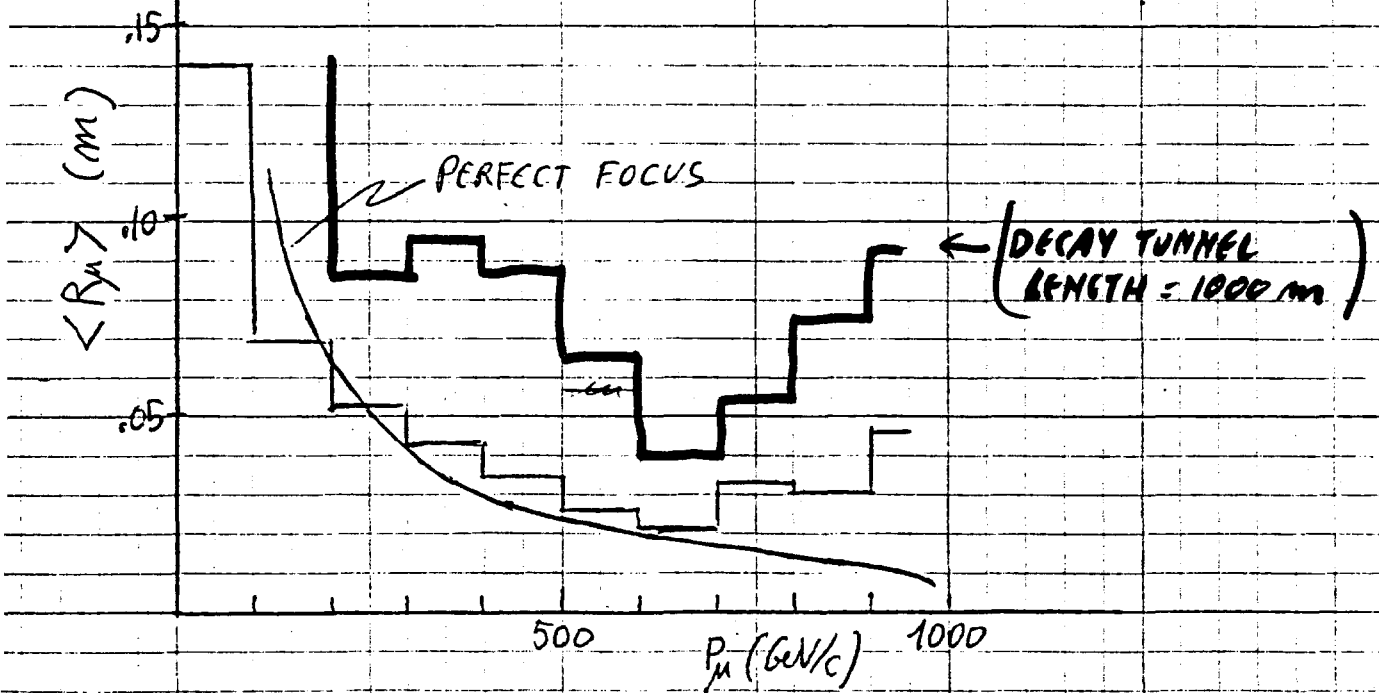
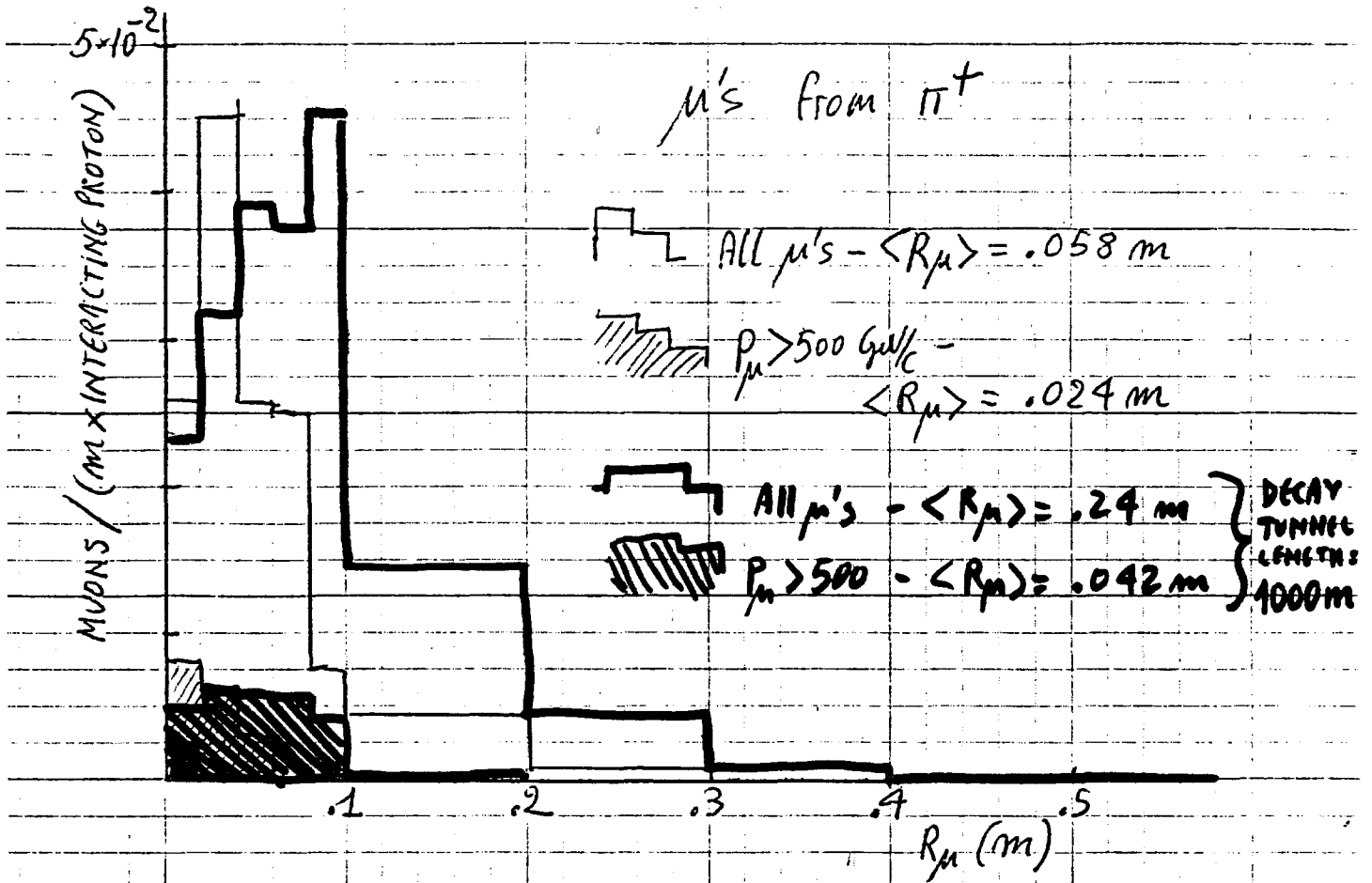
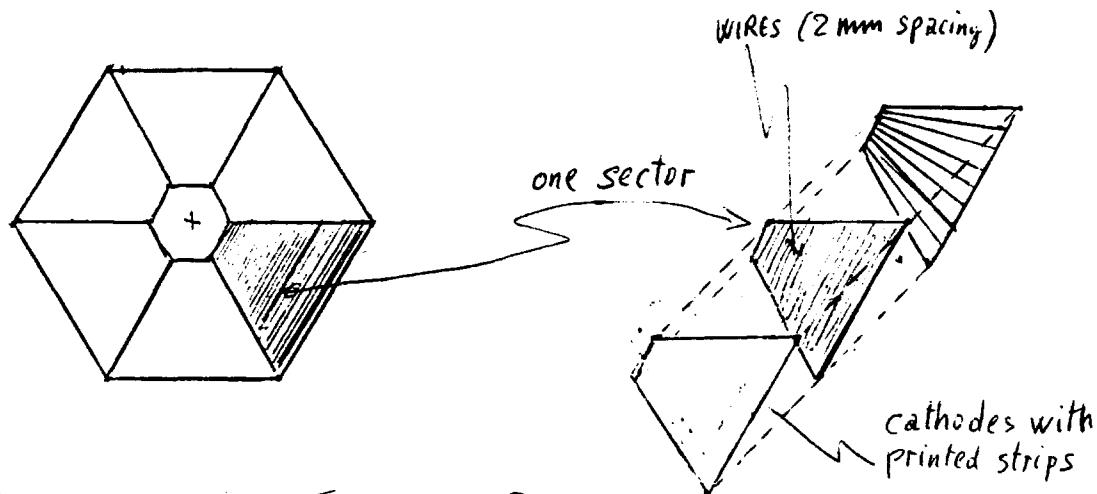
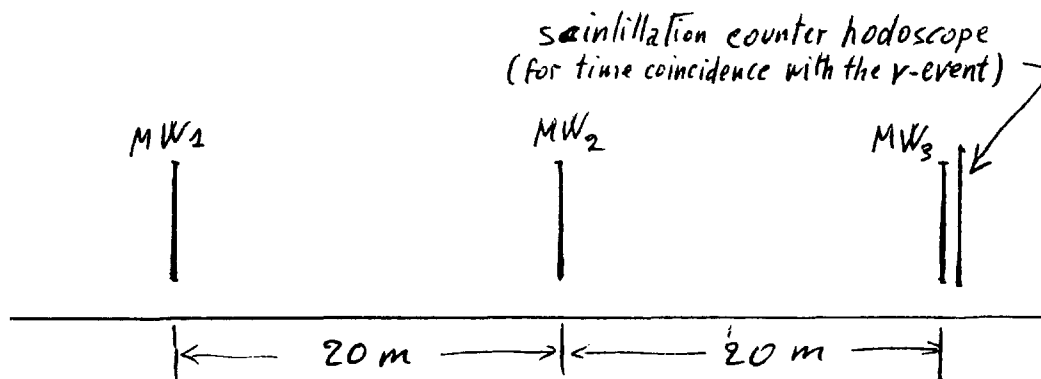
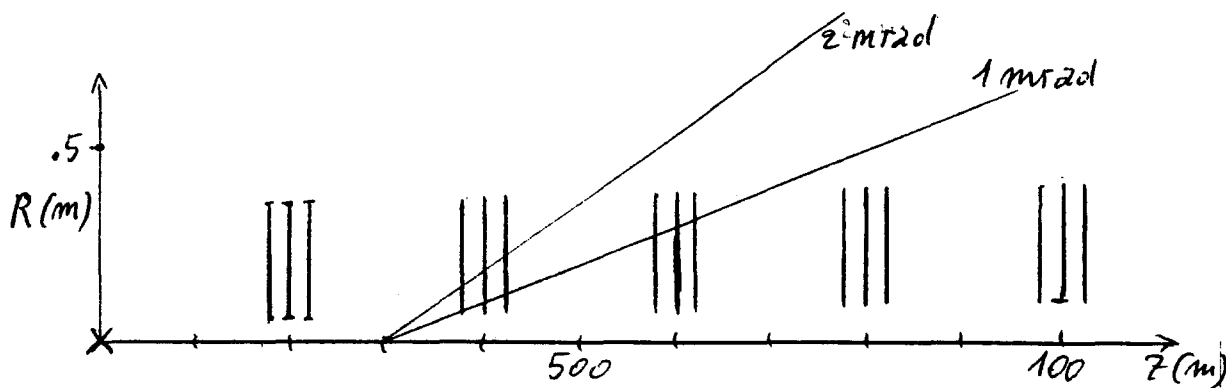


FIGURE 20



- 5 measurement stations
- 3 chambers } each station
- 1 hodoscope } each station
- 6 independent sectors each chamber
- 150 wires (2mm spacing) } each sector
- 50 cathodic strips } each sector

Total

- 27000 wire read-out
- 9000 strip read-out

FIGURE 21

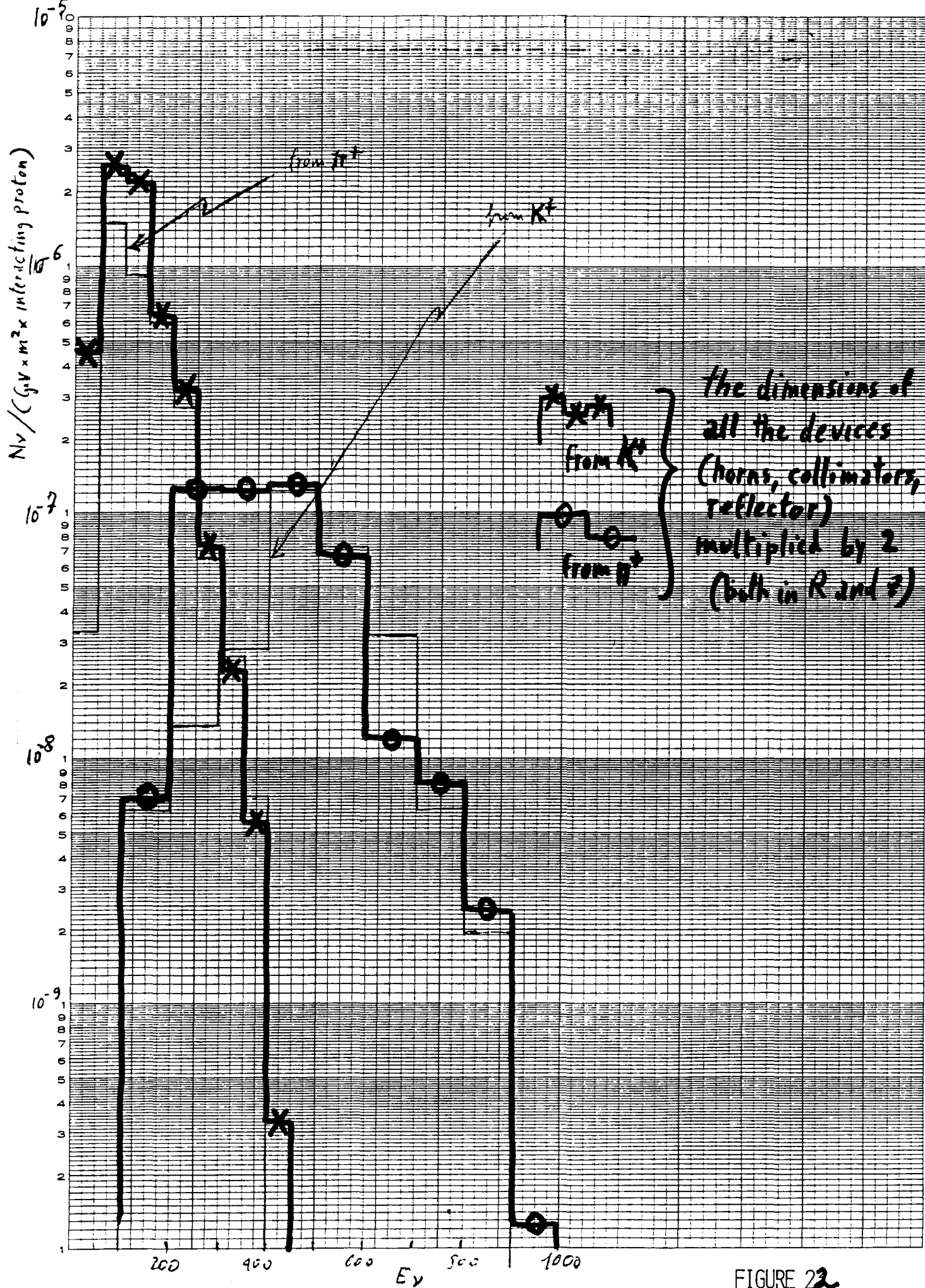
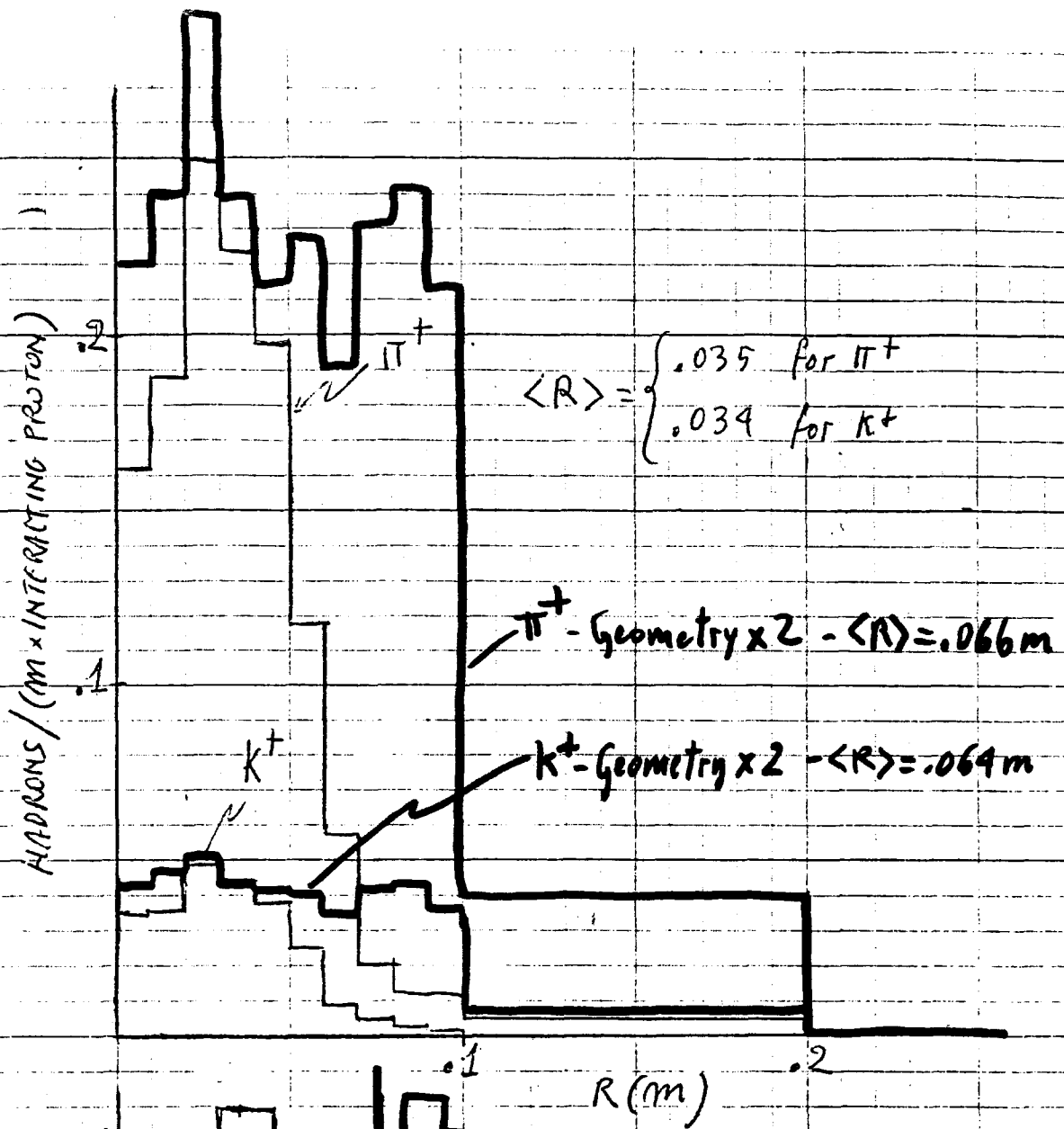


FIGURE 22

a)



b)

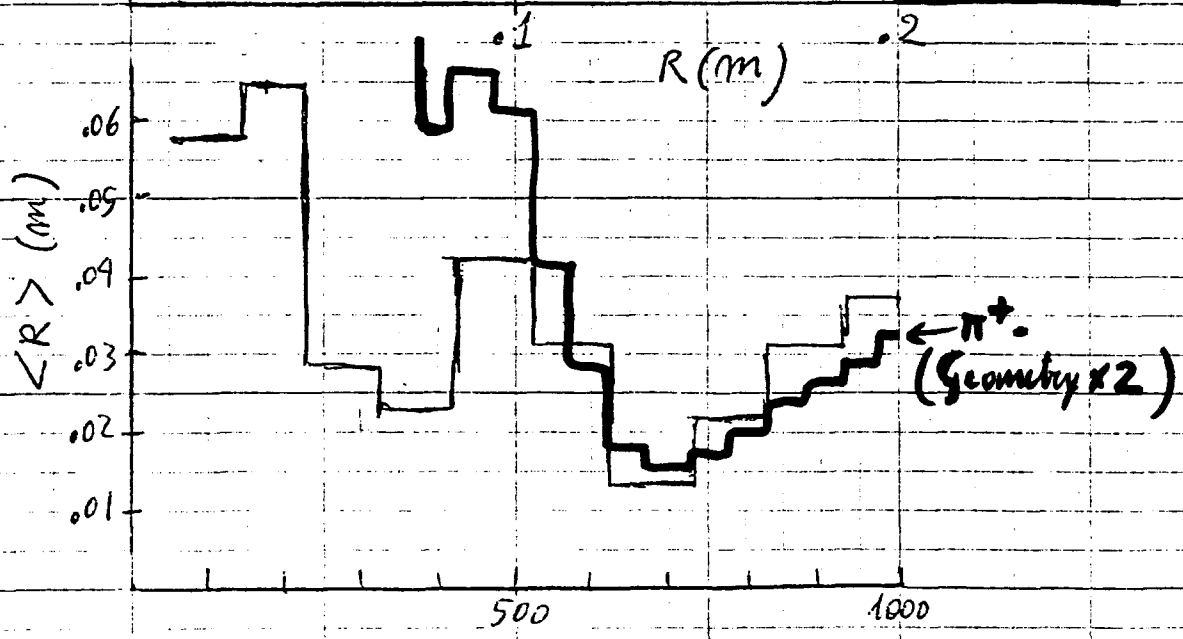


FIGURE 23

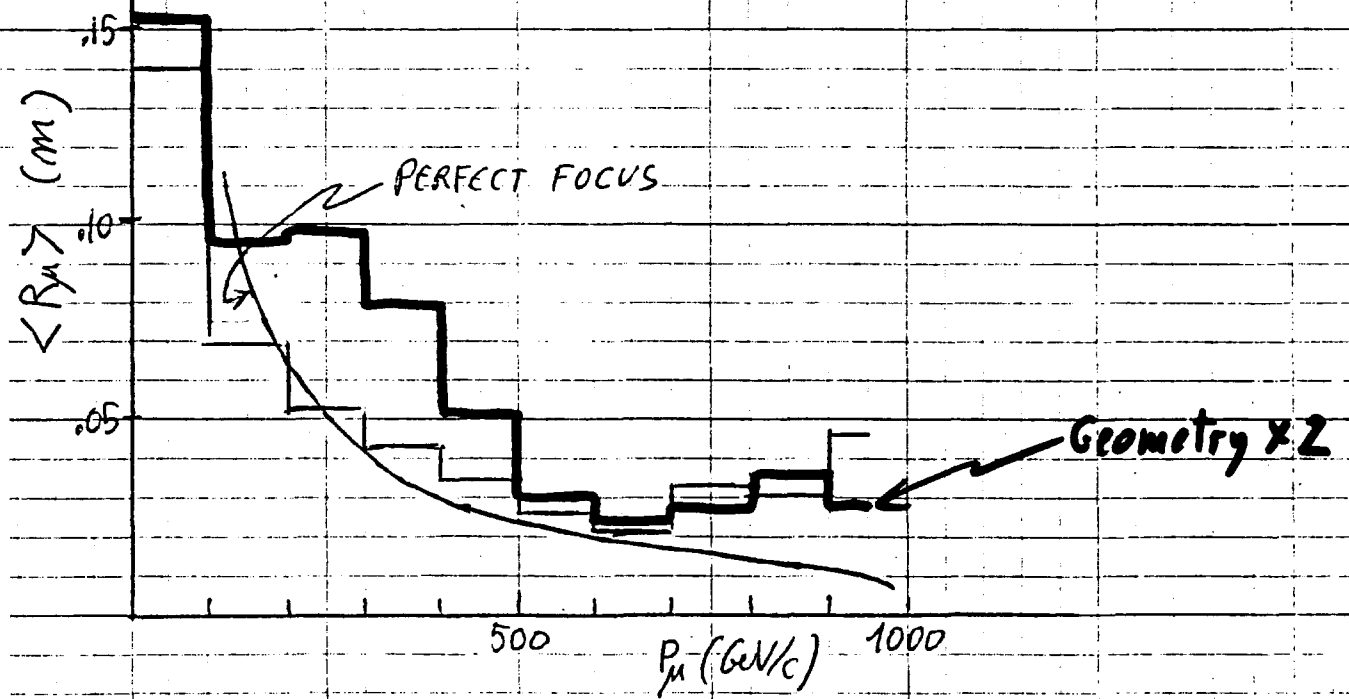
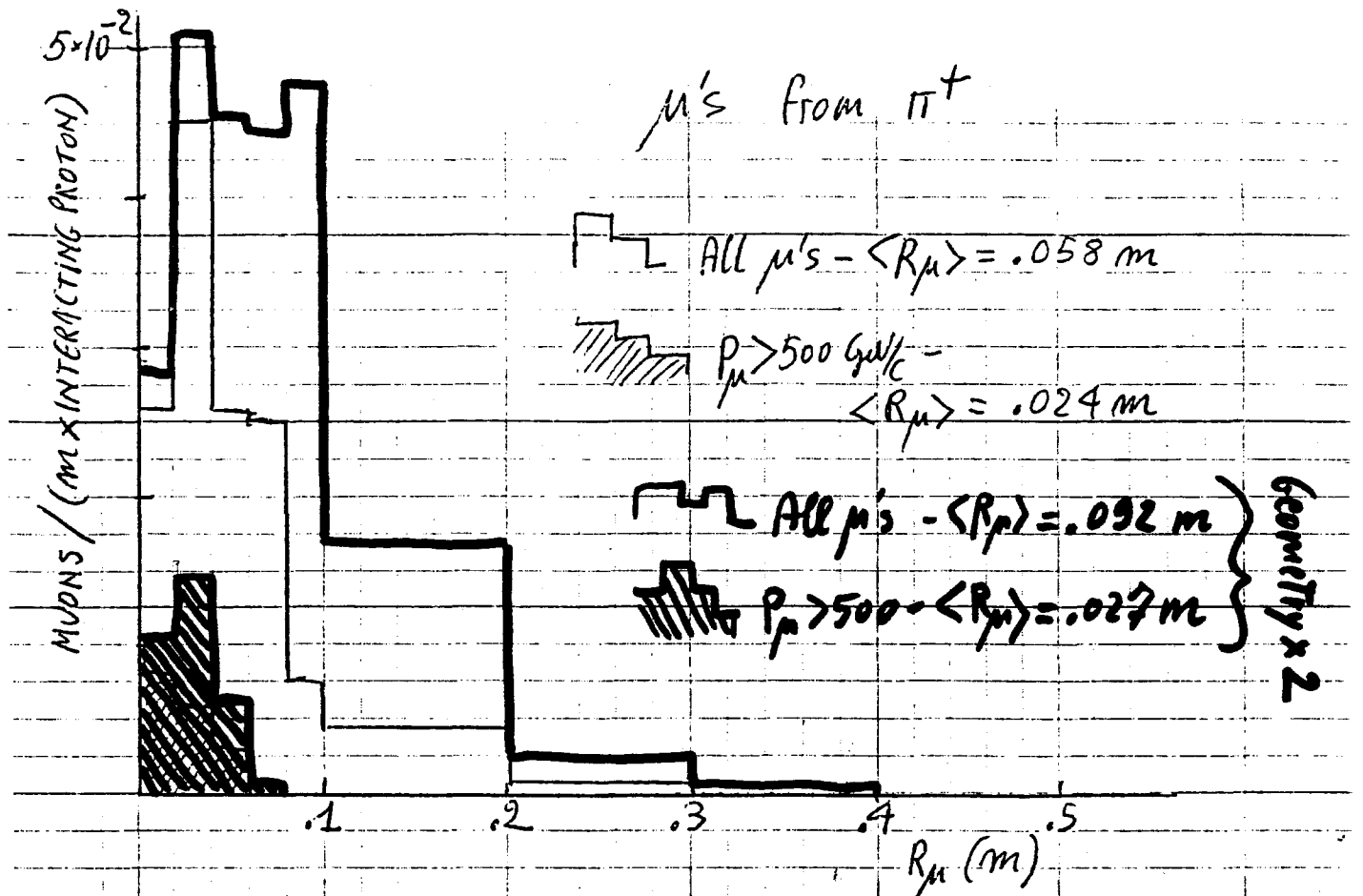


FIGURE 24

APPENDIX

Suppose we have at a distance Z_0 from a point source a circular lens, able to focus at infinity all particles emerging with momentum $p = \bar{p}$ (see Fig. A.1). The bending power of the lens must be proportional to the radius \bar{R} :

$$\frac{L(R) \times B(R)}{\bar{p}} = \frac{c \times \bar{R}}{\bar{p}}$$

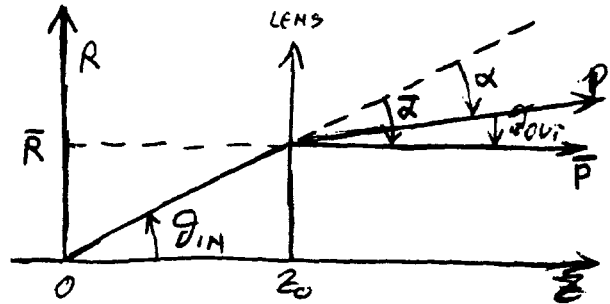


Figure A.1

If $L(R) \ll Z_0$ (thin lens approximation) particles with $p \neq \bar{p}$ emerge from the lens with a divergence

$$\theta_{out} = \theta_{in} - \alpha = \theta_{in} - \theta_{in} \frac{\bar{p}}{p} = \theta_{in} \times \left(\frac{p - \bar{p}}{p} \right)$$

since $\alpha \bar{p} = \bar{\alpha} \bar{p} = \theta_{in} \bar{p}$

The trend of the ratio $\theta_{out}/\theta_{in} = \frac{p - \bar{p}}{p}$ with p/\bar{p} is given by curve 1 Fig. 1 of the report.

If we have two thin circular lenses of opposite sign, the first at $Z_1 = Z_0$ and the second at $Z_2 = 1.5$, and the first one is focusing and the second one defocusing, with the notations of Fig. A.2 we have

in the I lens $\alpha_1 = \frac{\bar{R}_1 \bar{p}}{p}$ with $\bar{\alpha}_1 = \frac{c R_1}{\bar{p}}$
 in the II lens $\alpha_2 = \frac{\bar{R}_2 \bar{p}}{p} \times \frac{R_2}{R_1}$

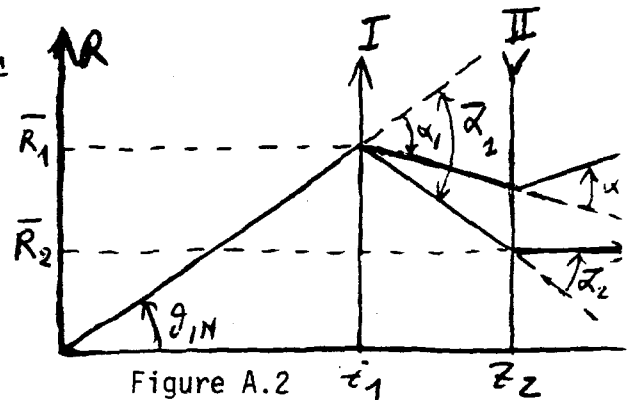


Figure A.2

For the particular geometry of Fig. A.2

$$R_2 = R_1 - (Z_2 - Z_1) \times (\theta_{in} - \alpha_1)$$

and hence

$$\alpha_2 = \frac{\bar{R}_2 \bar{p}}{p} \left(1 - \frac{Z_2 - Z_1}{R_1} (\theta_{in} - \alpha_1) \right) = \frac{\bar{R}_2 \bar{p}}{p} \left(1 - \frac{1}{2 \theta_{in}} (\theta_{in} - \alpha_1) \right)$$

$$\text{and } \alpha_{TOT} = \alpha_1 - \alpha_2 = \frac{\bar{R}_1 \bar{p}}{p} \left(1 - 1 + \frac{1}{2} \left(1 - \frac{\alpha_1}{\theta_{in}} \right) \right) = \theta_{in} \frac{\bar{p}}{p} \left(1 - 2 \frac{\bar{p}}{p} \right)$$

$$\theta_{out} = \theta_{in} + \alpha_{TOT} = \theta_{in} \left(1 + \frac{\bar{p}}{p} \left(1 - 2 \frac{\bar{p}}{p} \right) \right)$$